Journal of Structural Geology 178 (2024) 105009

Contents lists available at ScienceDirect

Journal of Structural Geology

journal homepage: www.elsevier.com/locate/jsg

Multiple compression directions and basinal response in a rhomb-shaped terrestrial basin: The Cuevas de Cañart syncline (Iberian Chain, eastern Spain)

Lourenço Steel Hart [a,b,*], Antonio M. Casas-Sainz [b], José L. Simón [b]

[a] Faculdade de Ciências, Instituto Dom Luiz, Universidade de Lisboa, Campo Grande, Edifício C1, Piso 1, 1749-016, Lisboa, Portugal
[b] Departamento de Ciencias de la Tierra, Grupo Geotransfer-IUCA, Universidad de Zaragoza. C/ Pedro Cerbuna 12, 50009, Zaragoza, Spain

ARTICLE INFO

Keywords:
Piggyback basin
Pull-apart basin
Thrust
Alpine compression
Tectono-sedimentary relationships

ABSTRACT

Rhomb-shaped basins have been commonly attributed to strike-slip tectonics, linked to fault bends and jogs (pull-apart basins). The case-study presented in this work (Las Cuevas de Cañart basin, Iberian Chain) is a 2 km × 5 km continental basin that shows a particular combination of geometric and sedimentary features. It shows a syncline geometry with steeply-dipping limbs, thickness of syn-tectonic sedimentary continental filling of about 1000 m, high amplitude/wavelength ratio, and different fold trends, some of them oblique to the main trend of the Iberian Chain. All these features make it an interesting case of a mixed-type basin, sharing both compressional and strike-slip features. The Cuevas de Cañart basin shows a Mesozoic, pre-compressional sequence linked to the extensional processes dominating in the marginal zones of the Maestrazgo basin, with a series up to 1500 m thick of limestones, sandstones and shales. These units overlie a detachment level (Upper Triassic Keuper facies) and show thickness variations controlled by NW-SE and NE-SW striking normal faults. During the Cenozoic compression, both fault systems were re-activated, and newly formed E-W folds (perpendicular to one of the dominant shortening directions) also appeared in the southern basin margin. The detailed structural study of this basin evidences the role of different types of structures (basement faults, thrusts formed under different compression directions) and the relevance of the detachment level in the evolution of compressional basins and thin-skinned fold-and-thrust belts.

1. Introduction

Rhomb-shaped basins are typical features of strike-slip-dominated tectonic settings (Basile and Brun, 1999; Okay et al., 1999; Einsele, 2000; Decker et al., 2005; Allen and Allen, 2013, among others). Interpretations for their origin range from simple pull-apart basins (Fig. 1a), associated with relay zones (Fig. 1b) or jogs (Fig. 1c) (Aydin and Nur, 1982, 1985; Biddle and Christie-Blick, 1985; Cunningham and Mann, 2007) to complex scenarios, with multi-stage evolution of paleostresses (Fig. 1d), under changing stress regimes and stress axes directions (Liu et al., 2013). In the latter case, many reported cases indicate that these basins underwent compressional and extensional stages, sequential or alternate, involving re-activation of faults formed during the different tectonic periods (e.g., Pannonian basin, Decker, 1996; Fodor et al., 1999; Falcón basin, Baquero et al., 2009; Sichuan basin, Yang et al., 2019). Specifically, zones of fault interference (Fig. 1e) between different structural trends are especially prone to the development of rhomb-shaped basins with a complex evolution, considering paleostresses and kinematics of basement structures (Muessig, 1984; Sun et al., 2003, 2004, 2006). Salt-tectonics studies have added new constraints for the interpretation of rhomb-shaped basins (Fig. 1f) (Smit et al., 2008; Teixell et al., 2017), both interpreting salt as the primary cause for basin subsidence (i.e. minibasins) or diapirs and other salt-related structures as features occurring in late stages of basin evolution.

Therefore, the study of rhomb-shaped basins must consider features related with fault reactivation and basin inversion. In many of the above-cited examples, compressional and strike-slip features combine to finally define the shape and evolution of sedimentary basins. Particularly, the interaction between strike-slip systems and thrusts determines the shape, drainage system and sedimentary regime (internally or externally-drained) of continental basins (Cobbold et al., 1993; Zhihong

* Corresponding author. Faculdade de Ciências, Instituto Dom Luiz, Universidade de Lisboa, Campo Grande, Edifício C1, Piso 1, 1749-016, Lisboa, Portugal
E-mail addresses: L.steel.Hart@gmail.com (L. Steel Hart), acasas@unizar.es (A.M. Casas-Sainz), jsimon@unizar.es (J.L. Simón).

https://doi.org/10.1016/j.jsg.2023.105009
Received 30 June 2023; Received in revised form 19 October 2023; Accepted 15 November 2023
Available online 24 November 2023

et al., 2009). The geometry of this kind of basins is associated with the structures formed at their boundaries, or within the basins themselves, segmenting them in different sub-basins (Cheng et al., 2021 and references therein). The interpretation of the mechanisms of basin formation becomes especially controversial when several folding directions are involved (Li et al., 2015), because they can be linked to different compression directions related to basin/orogen evolution (Rodríguez-Pascua and De Vicente, 1998; Simón, 2006a, 2019) or stresses transferred from the margins to the inner parts of the plates.

The Iberian Chain has been the subject of many geological studies. Its tectonic evolution, however, has not been completely understood, particularly when it comes to the interference patterns between different fold sets and their relationships with the compression directions in the Iberian microcontinent context, during the Paleogene and the Early Neogene (Guimerà, 1984; Casas-Sainz and Faccenna, 2001; De Vicente et al., 2007, 2009, 2018; Liesa and Simón, 2009; Martín-González and Heredia, 2011; De Vicente and Muñoz-Martín, 2013). Because of the preservation of syn-tectonic sediments associated with different tectonic trends, basins having syncline geometries in the inner sectors of the Iberian Chain can help to understand its kinematic evolution (e.g., Cuevas de Cañart basin, González et al., 1985; Aliaga basin, González and Guimerà, 1993; Simón, 2006a; Montalbán basin, Casas et al., 2000; Zaorejas basin, Rodríguez-Pascua and De Vicente, 1998).

This work focuses on the study of the Cuevas de Cañart (CC) syncline basin, a Cenozoic contractive alpine structure within the Iberian Chain that has not been analysed in depth from the structural point of view. Within the frame of the Iberian Chain, the CC syncline basin is particularly interesting, for different reasons. In this area, three structural directions co-exist: NE-SW (the most conspicuous one), N–S, and E-W, all of them with limited presence in the Iberian Chain compared to the prevailing NW-SE structural direction. Its Cenozoic sedimentary record provides interesting tectono-sedimentary relationships with those structures, which were previously studied by González et al. (1985). Because of this, and alongside with its size, shape, geographical location and easy accessibility, the studied area presents itself as a singular opportunity to study the different prevailing structures at each stage and their relationships with the compressional stress fields active during the Cenozoic. The CC basin can, therefore, be a source of data for interpreting other, more complex areas, either because of the strong deformation underwent by the rocks at their margins (Socquet and Pubellier, 2005; Morozov et al., 2014), outcrop conditions (i.e. offshore basins or basins underneath a recent sedimentary cover, Okay et al., 2000), because the main basinal features have been obliterated by subsequent compressional stages (Laville, 1988) or because of their dimensions, that do not allow for very detailed structural studies (Sun et al., 2003; Chen et al., 2019; Liu et al., 2021). In some of these basins, structures underlain by a basal *décollement* and different fold trends, as well as transport directions, are present.

Consequently, the main goal of this work is to characterize the structure of the CC syncline and propose an evolutionary model, consistent with its structural and sedimentary features. For this, seriated cross-sections, tectono-sedimentary and classical structural and paleostress analysis were used. As justified above, the conclusions and basin model proposed in this work can be applied to the interpretation of larger-scale basins in more complex, intraplate scenarios.

2. Geological framework

The CC basin is located in the Linking Zone between the Iberian and the Catalan Coastal Chains (Fig. 2). From the point of view of the Mesozoic basin evolution, the area is located within the Maestrazgo extensional basin, specifically in the Morella subbasin.

The Iberian Chain is an intraplate mountain range with an approximate NW-SE direction, and a moderate deformation style. Three main tectonic episodes contributed to build the Iberian Chain: the Permian-Mesozoic rift, the Alpine compression and the Neogene extension.

The first episode is associated with the propagation of the Northern Atlantic and the Tethysian rifts (Salas et al., 2001) and is responsible for some of the extensional basins that are found within the Iberian plate, such as the Maestrazgo Basin, (Martín-Chivelet et al., 2002). These basins were delimited by high-angle, NW-SE striking normal faults, articulated with low-angle, E-W to NE-SW trending ones (Álvaro et al., 1979; Soria et al., 2000), that belong to the Iberian rift system. The Maestrazgo basin underwent three rifting stages: (1) A first stage in the Permian/-Triassic, that was followed by a generalized thermal subsidence of the Iberian basin that, together with some eustatic fluctuations, was responsible for a marine transgression (Álvaro et al., 1979; Salas, 1987); (2) In the Late Jurassic to Early Cretaceous, associated with the opening of the Bay of Biscay (Álvaro et al., 1979), responsible for the division of this basin into different subbasins; (3) In the Late Cretaceous, associated with thermal subsidence throughout eastern Iberia. The Morella subbasin lies within the NW sector of the Maestrazgo basin, and is

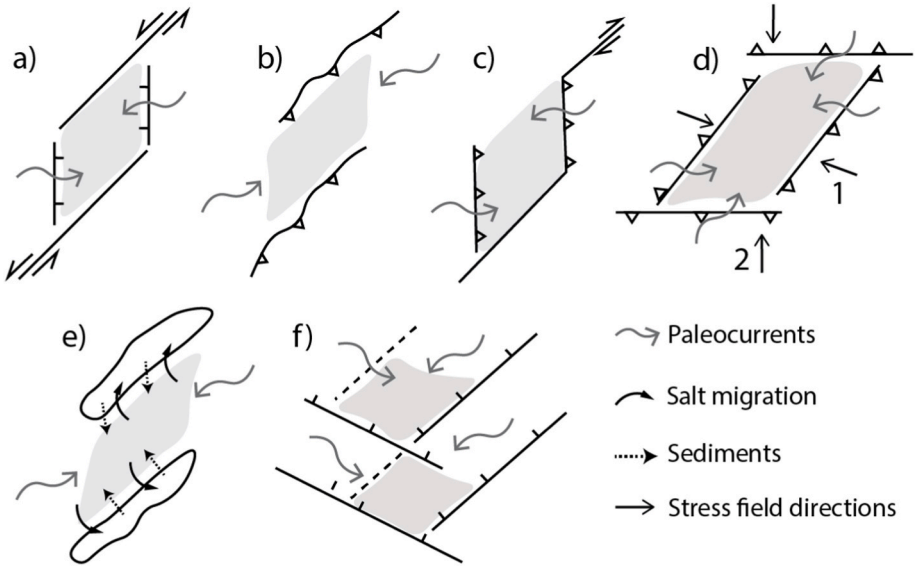

Fig. 1. Different methods of rhomb-shaped basins formation. (a) Pull-apart. (b) Relay compressional zones. (c) Migration of compressed jog (Foreland then Piggyback). (d) Successive compressional stress directions. (e) Fault interference. (f) Mini basin between relaying salt-walls.

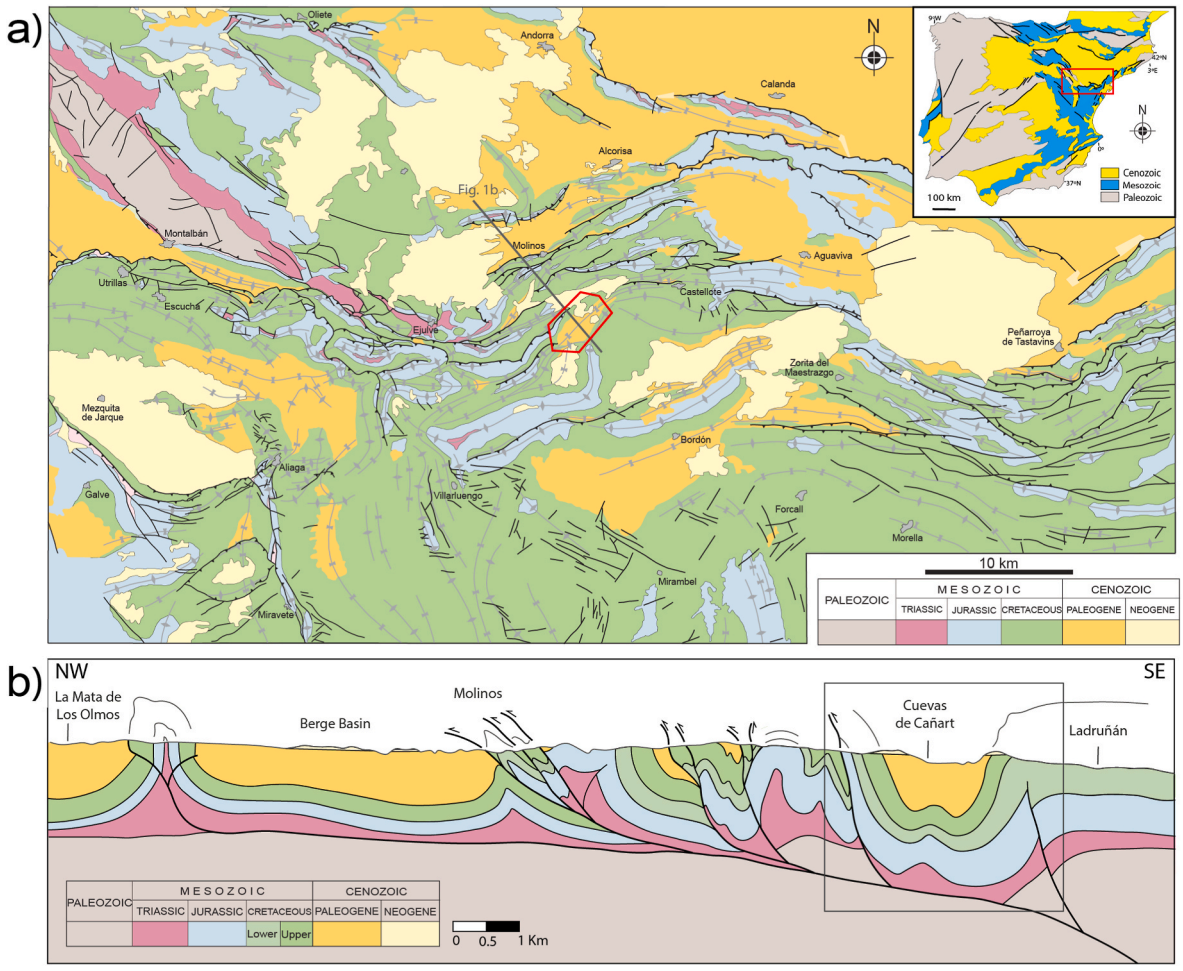

Fig. 2. a) Simplified tectonic map of the Linking Zone sector of the Iberian Chain, adapted from Simón et al. (2018), highlighting the study area. (b) Contextual cross-section of the area surrounding the Cuevas de Cañart syncline, within the Linking Zone. See location in (a).

controlled by listric ESE-WNW striking, southwards dipping faults (Salas and Guimerà, 1996; Antolín-Tomás et al., 2007; Nebot and Guimerà, 2016).

The second episode is dominated by the Alpine compression, dating from the Eocene to the mid Miocene. It produced the main structures found in this chain such as folds, thrusts and strike-slip faults with a prevalent NW-SE direction, while coeval NE-SW trending structures also developed locally in the Castilian Branch and the Linking Zone; all of them were subsequently overprinted by another series of WSW-ENE and E-W folds (Álvaro et al., 1979; Salas and Casas, 1993; Simón, 2004, 2005; De Vicente et al., 2009; Liesa, 2011; Liesa et al., 2018). Therefore, positive inversion of the extensional Mesozoic Iberian basin was caused by compression both normal (NNE to NE) and parallel (SE to SSE) to its boundaries (Liesa et al., 2018). The normal compression occurred during the Late Eocene to Late Oligocene, and was responsible for the main folds and thrusts. The parallel compression was especially significant during the Early Miocene, when the convergence between the Iberian and African plates were transferred from the Pyrenean to the Betic margin of Iberia (Liesa and Simón, 2009). The third and final tectonic stage is associated with the opening of the Gulf of Valencia during the Neogene-Quaternary, that originated multiple basins oblique to the Iberian Chain compressive structure (Álvaro et al., 1979; Capote et al., 2002).

The Iberian Chain can be divided into five main sectors: the Cameros unit, the Aragonese and Castilian branches, and the Levante and Maestrazgo sectors. At the northern Maestrazgo, the so-called Linking Zone (Guimerà, 1988) makes the connection with the Catalonian Ranges. In this last sector, we can find the study area, where the typical NW-SE trending structures of the Iberian Chain alternate with transverse, NE-SW (sinistral-reverse) trending structures that connect with those of the Catalan Coastal chains. It is also possible to find structures with an intermediate direction, approximately E-W, namely thrusts, facilitated by major basement faults with the same approximate direction. These faults are possibly pre-existent but, during the compression, they showed a predominantly reverse and later a strike-slip movement (Guimerà, 1984; Liesa et al., 2018). Some seismic profiles and boreholes indicate that some of these thrusts reach the Variscan basement (Salas et al., 2001). The northern part of the Linking Zone is characterized by a thin-skinned fold-and-thrust belt including low-angle thrusts, detached at the middle Muschelkalk evaporitic facies (Vegas et al., 2019). Several synorogenic, isolated basins developed within this fold-and-thrust belt (Cuevas de Cañart, González et al., 1985; Aliaga, González and Guimerà, 1993; Montalbán, Casas et al., 2000), thus constituting a useful record of the Alpine contractive evolution.

According to the model by Liesa and Simón (2007, 2009), the regional distribution and time relationships of the different compression directions recorded within the Iberian Chain, together with the consideration of their geodynamic setting, allow defining three independent intraplate stress fields: *Iberian*, *Betic*, and *Late Pyrenean*. They were originated by distinct combinations of forces transmitted from the Iberian plate margins, mostly by a composite of the Mid Atlantic ridge push and the convergence at either the Pyrenean or the Betic boundary. These stress fields were active during Cenozoic times, evolving through four main compressional stages (Liesa and Simón, 2009; Simón, 2006a,

2019b): (1) *Early Betic* (WNW-ESE, Eocene-Early Oligocene in age); (2) *Iberian* (NE-SW to ENE-WSW; Oligocene); (3) *Late Betic* (NNW-SSE; Oligocene-Miocene transition), and (4) *Late Pyrenean* (NNE-SSW; Early Miocene).

Alternative tectonic models have been proposed suggesting the action of a single N–S to NNE-SSW compression (orthogonal to the direction of the Pyrenees) throughout the Palaeogene (e.g., Guimerà, 1988; De Vicente et al., 2009). According to those models, the plurality of directions of contractive structures within the Iberian Chain would be a consequence of different processes: (i) local deformation conditions at restraining and releasing steps or at fault relays within strike-slip fault zones; (ii) stress deflection at compressional and extensional fault tips (mostly in strike-slip faults); (iii) strain partitioning processes under constrictive or transpressive deformation regimes. This issue will be taken up again in the Discussion section below.

3. Methodology

To achieve the above-mentioned objectives, different techniques were applied, including observation of aerial photographs with stereographic superposition and orthophotographs (processed by means of Qgis and GoogleEarthPro). To better understand the structure of the CC area, and to improve the existing geological map, the sector (15 km^2) was mapped in detail at a 1:15,000 scale (Fig. 3b), paying special attention to faults, folds and stratigraphic relationships. Field work was oriented towards observation of lithological boundaries and structures on an outcrop scale, and collecting orientation data of bedding (Fig. 3a), angular unconformities, fault planes and slickenlines, fold hinges, and pressure-solution lineations.

All these data were analysed and interpreted during the third and final stage. The main structure was represented through geological cross sections, and the orientations of structures in detail (fault planes and slickenlines, fold hinges, pressure-solution lineations) were plotted by using Stereonet (Allmendinger et al., 2011; Cardozo and Allmendinger, 2013).

Fault planes and slickenlines were additionally subjected to paleostress analysis using two robust methods: Right Dihedra (Angelier and Mechler, 1977) and Etchecopar's method (Etchecopar et al., 1981). Application of other, more recent techniques was not considered, either by their intrinsic complexity (e.g., Yamaji, 2000; Sato and Yamaji, 2006), or because they essentially work as the latter do (e.g., Mostafa, 2005). It is true that some modern methods integrate friction criteria within the paleostress inversion procedure itself (e.g., Žalohar and Vrabec, 2007; Kaven et al., 2011), while Etchecopar's method considers mechanical constrains only *a posteriori*, once the optimum deviatoric stress tensor satisfying the Wallace–Bott's principle has been calculated. Nevertheless, the inversion process is essentially the same for all of them. In any case, all the precautions that some review articles have called for rigorous application of paleostress inversion (e.g., Hippolyte et al., 2012; Lacombe, 2012; Simón, 2019a) were taken into account: accurate data collection, critical assessing of the structural context, or careful treatment of poliphase fault-slip samples.

Mean orientations of solution lineations within each local sample (calculated with Stereonet) were taken as the best approach to obtain the orientation of local σ_1 axes (Simón, 2006b, 2007). In cases of polyphase samples, the mean orientation was calculated for each separated subsample after identifying it within the overall density diagram.

4. Stratigraphy of the study area

The stratigraphic series involved in the CC syncline includes units from the Late Triassic to the Early Neogene (Fig. 3). The Late Triassic is represented by the Keuper facies, exposed nearby, which consists of clays and green to red shales (Gómez and Goy, 1979). The marine Jurassic is represented by: (i) the Cortes de Tajuña Formation (100 m of brecciated dolostones, Upper Triassic to Lower Jurassic in age); (ii) the Cuevas Labradas, Barahona and Turmiel Formations, a 175 m thick calcareous and marly sequence, Lower Lias in age and rich in fossils (Gómez and Goy, 1979; Gómez et al., 2003); (iii) the Middle Jurassic Chelva Formation (170 m thick), composed of limestones and dolostones with chert nodules, and bioclastic limestones; (iv) the Upper Jurassic Loriguilla and Higueruelas Formations (150 m thick), made of carbonate-marls rhythmite followed by massive limestones (Aurell et al., 2019).

The Lower Cretaceous (pre-Albian) is represented by a continuous series between the La Pleta and Escucha formations (Canérot et al., 1982; Margarit, 2019). Both the upper and lower limits of this ensemble are angular unconformities, and its total thickness approximately reaches 800 m. Unconformably overlying this sequence, the Utrillas Formation (Albian in age in this sector) consists of layers of multicoloured, poorly compacted sand and sandstones (from white and yellow to red and brown), alternating with multicoloured clay levels (Canérot et al., 1982). Its average thickness is about 200 m, which decreases towards the South, locally disappearing under the Upper Cretaceous Mosqueruela Formation.

The Upper Cretaceous marine sequence is about 500 m thick and consists of well-bedded white limestones (Mosqueruela Fm.), massive dolostones (Barranco de los Degollados Formation, well-bedded, brecciated grey to white limestone layers (Organos de Montoro Fm.), alternating marls and limestones (La Cañadilla Fm.) and finally heavily brecciated dark continental limestones with thick grey marlstone levels (Fortanete Fm.) (Canérot et al., 1982).

The syn-compressional tecto-sedimentary units T1, T2, T3, T4 and T5 include Cretaceous levels at its base, followed by a 700 m thick sequence of conglomerates, sandstones, and mudstones/clays (González et al., 1985; González, 1989) with occasional limestones. They are separated by angular unconformities at the basin border and their corresponding sedimentary discontinuities towards the basin centre. In the absence of palaeontological dating, its age has been approached by González et al., 1985) by regional correlation with other dated basins. This correlation is based on the identification of those discontinuities and the sequential analysis of stratigraphic units (Pardo et al., 1989), and has been successfully achieved for the ensemble of basins representing the transition between the Iberian Chain and the Ebro Basin (González, 1989; Pérez, 1990; González and Pérez, 2018).

- The T1 unit would possibly correspond, according to González (1989), to a thin layer of red clays that crop out only at the northern limb of the main structure, overlying marine Cretaceous limestones. Because of its low thickness we have not distinguished it in maps and cross-sections.
- T2 (middle-late Eocene in age) crops out at the southern and northern limbs of the main syncline, reaching a maximum of 25 m in thickness. Its conglomeratic base represents a sedimentary rupture onto the marl deposits of the Fortanete Formation and T1 unit.
- T3 (late Eocene-early Oligocene) crops out at the centre of the syncline, occupying its core and reaching a maximum thickness of 470 m. It lies onto the T2 unit, and partially on the Fortanete and La Cañadilla Formations through an angular unconformity, while it has an onlap geometry towards the E.
- T4 (middle-late Oligocene) lies onto the T3 unit, as well as on several of the Cretaceous ones. It crops out at the centre of the syncline and reaches an approximate thickness of 120 m. Both its lower and upper limits are angular unconformities and, locally, the upper limit consists of a syn-tectonic unconformity.
- T5 (early Miocene) crops out attached to both the northern and southern limbs of the main syncline, with maximum thickness of approximately 70 m. It makes an angular unconformity with the previous units.

Finally, there is an unequal distribution of Quaternary deposits that include detrital alluvial sediments associated to a small piedmont on the

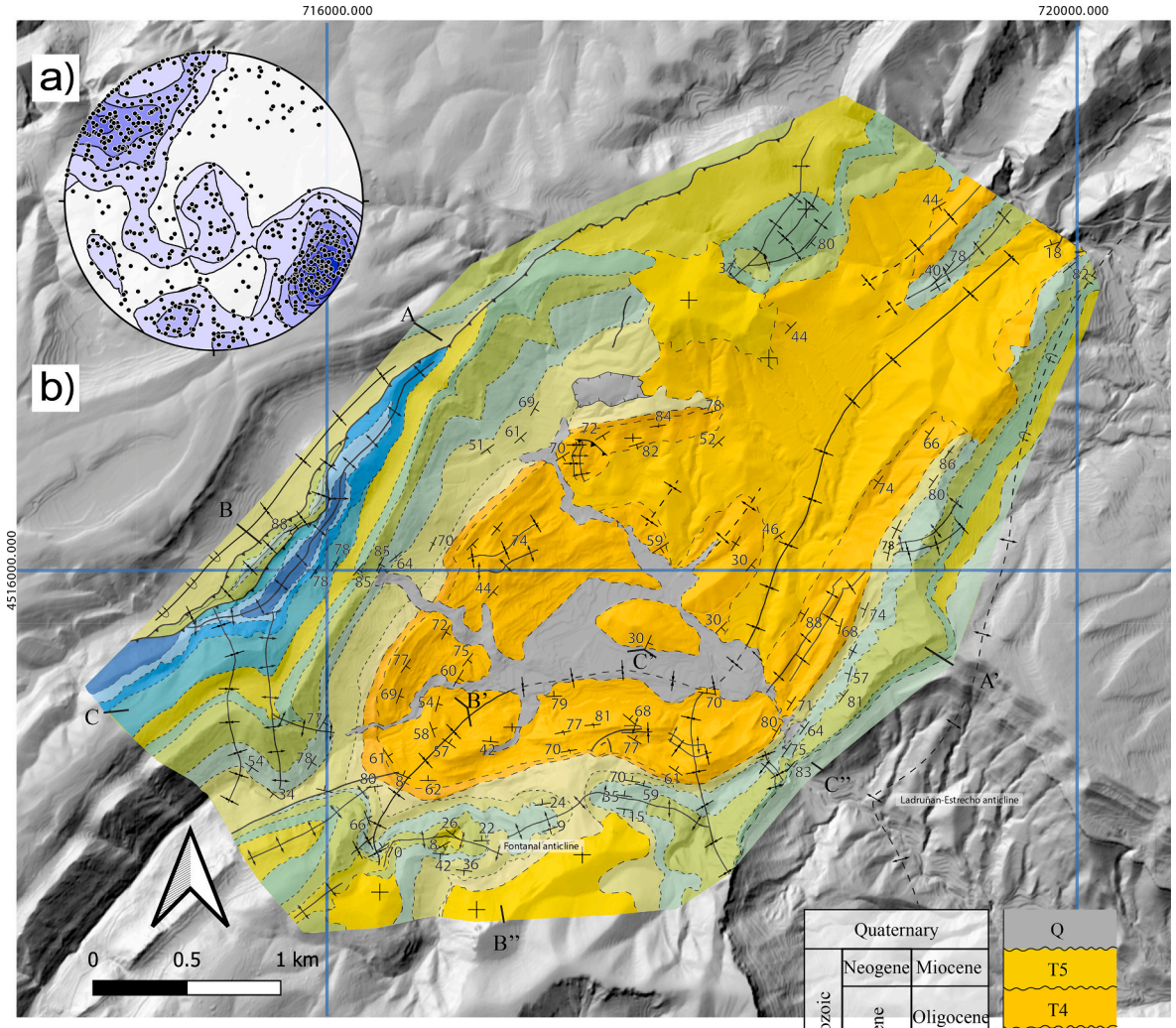

Stratigraphic contacts

- Conformable
- Unconformable

Bedding

- Horizontal
- Vertical
- Normal dip
- Inverted

Structures

- Anticline
- Sinclyne
- Recumbent syncline
- Recumbent anticline
- Fault
- Thrust

Units

Q: Quaternary deposits
T5: Neogene continental unit
T2, T3, T4: Paleogene continental units
C7: Fortanete Fm.
C6: La Cañadilla Fm.
C5: Órganos de Montoro Fm.
C4: Barranco de los Degollados Fm.
C3: Mosqueruela Fm.
C2: Utrillas Fm.
C1: Weald and Urgon facies
J5: Loriguilla and Higueruelas Fms.
J4: Chelva Fm.
J3: Turmiel Fm.
J2: Cuevas Labradas and Barahona Fms.
J1: Cortes de Tajuña Fm.
K: Keuper facies
TP: Middle and Lower Triassic + Paleozoic basement

Quaternary			Q
Cenozoic	Neogene	Miocene	T5
	Paleogene	Oligocene	T4
			T3
		Eocene	T2
Mesozoic	Cretaceous	Upper	C7
			C6
			C5
			C4
			C3
		Lower	C2
			C1
	Jurassic	Upper	J5
		Middle	J4
			J3
			J2
		Lower	J1
	Triassic		K
Paleozoic			TP

Fig. 3. a) Synthetic stereoplot of poles to bedding in the whole study area, with density contours. (b) Detailed geological map of the Cuevas de Cañart synclinorium.

northern limb of the CC syncline, as well as colluvium and an important tuff system. These deposits also cover unconformably the previously described units.

5. Macrostructures

5.1. Overall structure based on map and cross-sections

To reconstruct the main structure, and the multiple structures found within, three cross-sections (Fig. 4) were drawn based on the map of Fig. 3b. In these cross sections, both the Jurassic limestones and the carbonate Upper Cretaceous units were considered to have parallel contacts and constant thickness. For the remaining units (Fortanete Fm. and the Cenozoic units), containing a significant proportion of mudstones, an increase in thickness at the hinge of folds is accepted. Conversely, changes in thickness in the Lower Cretaceous (in general sedimentary wedges opening towards the East and South) units are often considerable, and related to the extensional features associated with the margin of the Maestrazgo basin.

The overall structure of the CC basin is an asymmetric brachysyncline (Fig. 4b) with a SW-NE direction (see the synthetic strereoplot of bedding poles in Fig. 3a) and NW vergence. It involves Cretaceous and Jurassic units at its limbs and the Cenozoic units at its core. The syncline has an approximate amplitude of 1200 m and an approximate wavelength of 6000 m.

In its northern limb, the structure is controlled by a double thrust system (Fig. 3b and 4b). The upper thrust affects both the Cretaceous and Jurassic units and has approximately 400 m of estimated net slip and crops out in a sub-vertical attitude. Its footwall is structured as a very tight, symmetric syncline, with the Órganos de Montoro Formation at its core and two sub-vertical limbs. The lower thrust affects the same units with an approximate slip of 100 m, and has an approximate dip of 60° S. Its footwall is characterized by an asymmetric syncline, with the La Cañadilla Formation at its core and a NW vergence, which can be locally described as a recumbent fold (Fig. 5b). In this limb, an angular unconformity, with the Mosqueruela Formation directly lying on top of different Jurassic units (Chelva, Loriguilla and Higueruelas Formations), is visible. The entire Lower Cretaceous is missing and the Upper Cretaceous units have in general a higher thickness than when compared with the southern limb, where locally neither the Fortanete, nor the Utrillas and Mosqueruela Formations crop out (Fig. 3b). These units dip between 50° and 90° towards south, and are locally overturned.

To the SE and to the S, the CC syncline is bounded by the Ladruñán-Estrecho anticline (Fig. 5a, d) (Margarit, 2019) and the Fontanal anticline (Fig. 5c), respectively.

The Ladruñán-Estrecho anticline can be divided into two main sectors: (1) Northern sector, with a N–S direction, slightly curving towards its northern tip. It is an asymmetric, west-verging anticline with Upper Cretaceous strata dipping 45°W in the western limb (Fig. 5a) and 5-10°E in the eastern one. The structure also presents a periclinal closure to the north, and a graben structure at its hinge, composed of NW-SE faults, dipping towards NE and SW. There is also an evident post-rift unconformity, with the Mosqueruela Formation lying directly on top of both the Utrillas Formation and the Lower Cretaceous sequence (Fig. 4a) (Margarit, 2019). Locally, it shows a recumbent geometry (Fig. 5b). (2) South-western sector, with an ENE-WSW direction and affecting the

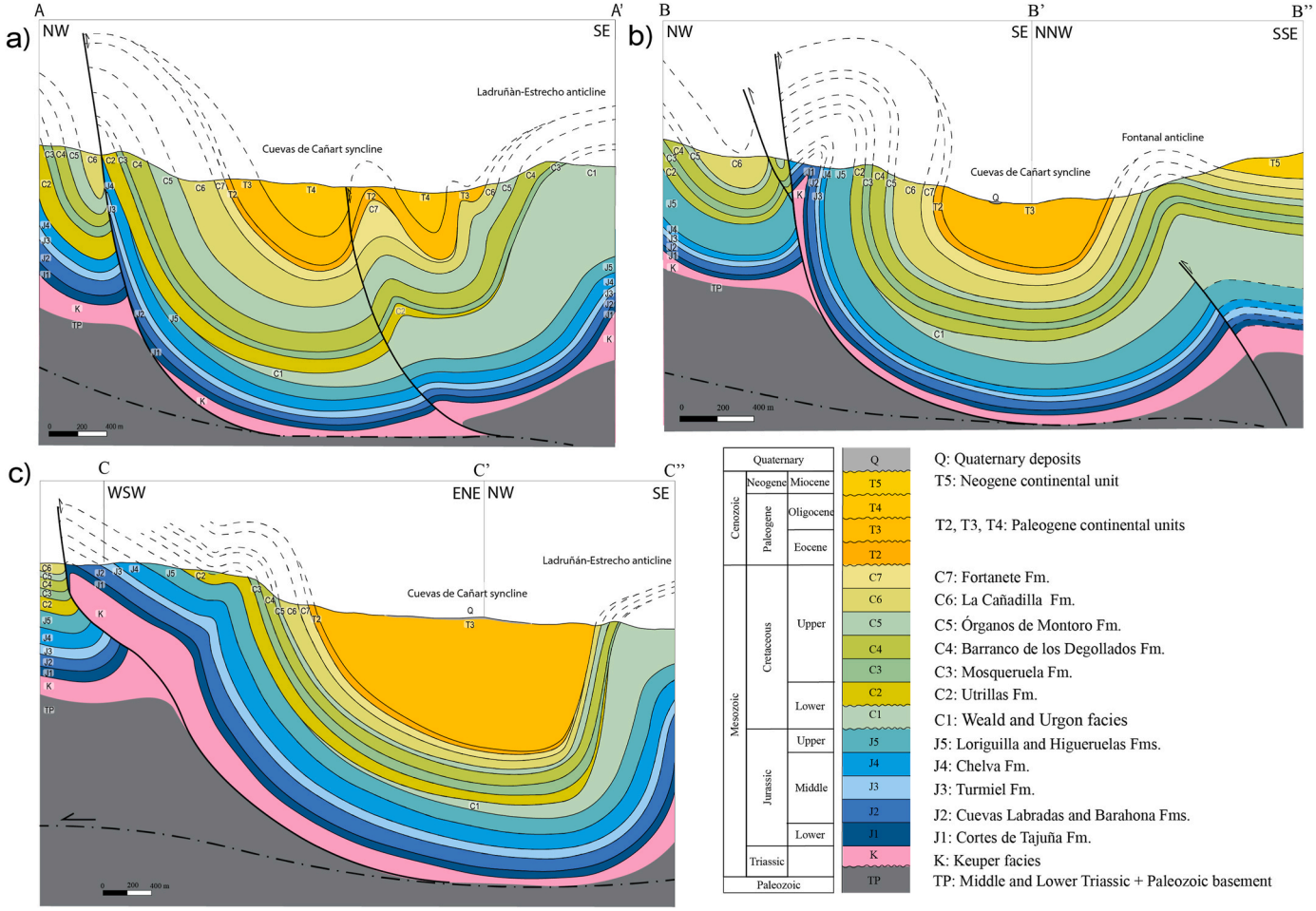

Fig. 4. Cross-sections of the of the Cuevas de Cañart synclinorium (see location, A-A′, B–B′ and C–C′, in Fig. 3b).

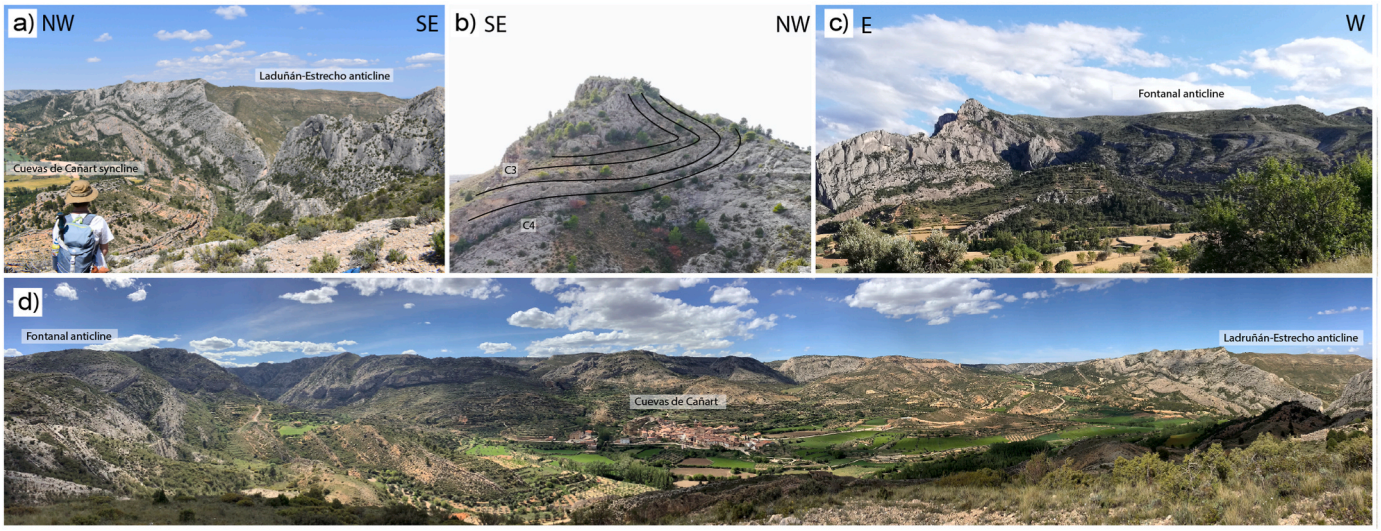

Fig. 5. Field view of macrostructures. (a) Connection between the Ladruñán-Estrecho anticline and the Cuevas de Cañart syncline. (b) Hinge of the Ladruñán-Estrecho anticline at the NE corner of the area mapped in Fig. 3b, locally showing a recumbent geometry. (c) Fontanal anticline, south of the CC syncline. d) Panoramic view of the CC syncline.

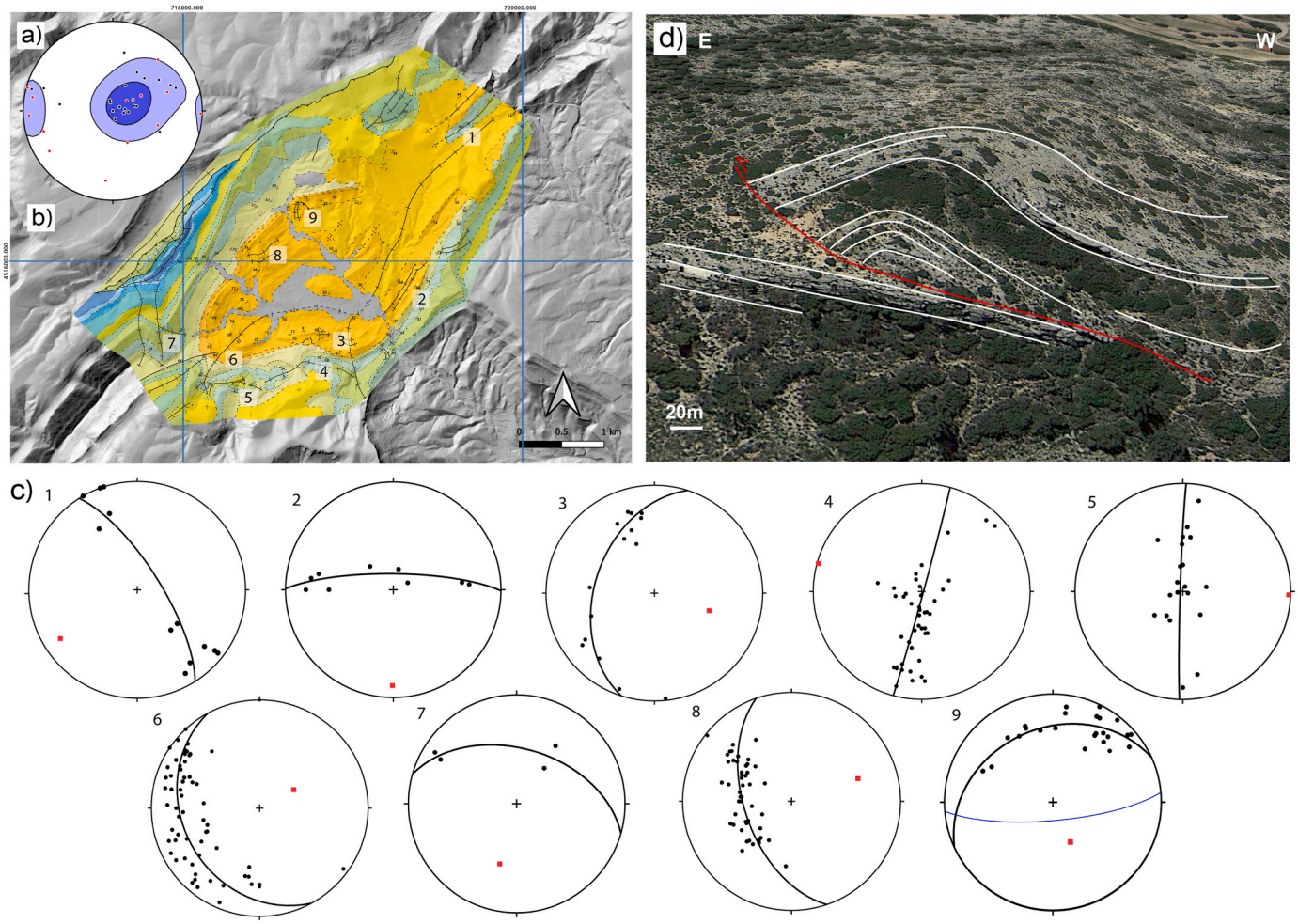

Fig. 6. a) Synthetic stereoplot with all the measured (in black) and inferred (in red) fold hinges within the Cuevas de Cañart area. b) Location map of the surveyed folds. (c) Stereoplots showing poles to bedding (black dots) and axes of individual folds (red dots). (d) Satellite image showing a NE-SW striking thrust and its associated hanging-wall anticline, both affecting the T3 unit close to the northern limb of the Cuevas de Cañart syncline (source: Landsat Copernicus, taken from Google Earth). (For interpretation of the references to colour in this figure legend, the reader is referred to the Web version of this article.)

Ladruñán and Herbers Formations. It is an asymmetric, north-verging fold with a subhorizontal axis and an axial plane dipping about 70°S (the north-eastern limb is nearly vertical, while the south-eastern limb has a gentle dip).

The Fontanal anticline (see Figs. 4b and 5c) shows an irregular axial surface with an approximate E-W direction. It is a segmented asymmetric fold, with a sub-horizontal southern limb and up to a 70°N dip in its northern limb. It affects the Cretaceous units, and separates the Miocene materials mapped to the south from the Cenozoic units of the CC syncline.

In the SE limb of the CC syncline, corresponding to the NW limb of the Ladruñán-Estrecho anticline, the deposition of the Cretaceous units was controlled by a blind fault (Castellote-Herbers Fault). This normal fault is responsible for the thickness variation of both the Lower and Upper Cretaceous, whose units approximately double their thickness to the south with respect to those at the studied area (Nebot, 2016). The fault was later inverted during the Paleogene, also nucleating the Fontanal anticline (see Fig. 4b).

The thrust system, depicted in Fig. 4b and c, shows a ramp geometry in both walls and is responsible for the two footwall synclines and the hanging wall anticline, depicted in the same figure. The whole structure is detached at the Keuper facies and reaches the basal décollement at a 2.5–3 km depth, where it tends to become horizontal. Basement steps, some of them inherited from the extensional stage, also account for the different vertical position of the Jurassic in the different blocks.

The Cenozoic pocket reaches approximately 1 km in thickness and is faulted at its core by a Paleogene thrust (Fig. 4b). The angular unconformities (Upper Jurassic-Lower Cretaceous, Lower Cretaceous-Utrillas Formation, Utrillas Formation-Mosqueruela Formation, Fortanete Formation-T2, T2-T3, T3-T4, T4-T5), are also observable in the cross-sections.

5.2. Directional analysis of folds

One of the most characteristic features of the CC basin is the presence of a variety of structural trends in a relatively small area. Throughout the CC syncline, both the Mesozoic and Cenozoic units are affected by three sets of structures: SW-NE, N–S and E-W (Fig. 6). These different sets will be described, separately.

The NE-plunging set has the clearest expression, out of the three (Fig. 6a). The CC syncline, as a whole, belongs to this set. In its two limbs, it is possible to find both Cenozoic and Mesozoic overturned layers (thus defining at places a teardrop fold geometry). In the southern termination, its hinge plunges 61° towards the NE, and its limbs dip between 50 and 70° (site 6 in Fig. 6c). Closer to its hinge, it is possible to observe some subvertical minor folds affecting the T3 limestone strata.

On the southern limb of the CC syncline, there is a syncline-anticline structure (2 in Fig. 6c) affecting the T3 unit. The fold axis plunges 23° towards the S and the structures verge towards the E. On the northern limb, there is also a northwards verging syncline-anticline structure (8 in Fig. 6c), with the fold axis plunging 36° towards the NW.

The N–S set affects most of the units as well, but it is not so well represented as the first one (7 and 9 in Fig. 6c) The N–S anticline that crops out in the western corner of the study area (7 in Fig. 6c) is a box fold that affects both the Cretaceous and Jurassic units, with an eastern limb dipping 54°W, a southern limb dipping 78°S and a western limb dipping 77°S.

Also with a N–S orientation, there is an asymmetric anticline-syncline structure (9 in Fig. 6c), verging towards the NE and plunging 60° towards the SE, that affects the T3 unit and covered by the T4 unit. It is associated with a NW-SE folded thrust (Fig. 6d), which is the only one in this sector with this direction (after restoring bedding to the pre-folding, post-thrusting position), typically associated with the dominant structural trend of the Iberian Chain. Though small, it separates two portions of the T3 unit, one deformed by N–S folds and the other not affected by them. No indicators of the direction of movement were found in situ.

The third set of structures, with an E-W orientation, mostly appears in the southern limb of the CC syncline (3, 4 and 5 in Fig. 6b). The first structure (3 in Fig. 6b) is a symmetric anticline-syncline pair affecting the T3 unit, whose axis plunges 46°E. Therefore, the T3 unit is affected by both N–S and E-W folds. Finally, a large E-W trending fold (Fontanal anticline), mostly visible in the Upper Cretaceous units, makes the southern margin of the CC basin. Its trace is divided into two slightly separated segments (4 and 5 in Fig. 6b), both showing a horizontal axis, a nearly horizontal southern limb and a northern limb dipping about 80°N.

6. Tectono-sedimentary relationships

The tectonic framework of a basin, as well as its structural evolution, can be reconstructed through a careful analysis of the geometrical and chronological relationships between the successive sedimentary units, and the faults and folds that bound the basin or deform its infill. This is especially true for the small continental, synorogenic basins developed within fold-and-thrust belts. Within the Iberian Chain and the transition towards the Ebro Basin, such tectono-sedimentary analysis has allowed reconstructing the evolution of the main basins, both in compressional and extensional settings; e.g., Aliaga (González, 1989; González and Guimerà, 1993), Montalbán (Pérez, 1990), Teruel (Ezquerro, 2017; Ezquerro et al., 2019), El Pobo (Simón-Porcar et al., 2019).

In the case of the CC basin, the relationships between tectonic structures and sedimentary units are best expressed at the basin margins, where unconformities are usually found. Unfortunately, the outermost sectors of the units, out of the present-day synclinorium, have been eroded and therefore only some of these tectono-sedimentary relationships can be inferred.

Firstly, the ensemble of T2 and T3 units overlie the Mesozoic units of both the southern and the northern limbs of the main syncline showing onlap geometry (see map of Fig. 3b). This indicates that uplifting of both limbs initiated during the first deformation stages, prior or coeval to deposition of T2. This inference is consistent with the interpretation by González et al. (1985), who established that T2 has its source area to the SE, at the neighbouring Ladruñán anticline, already emerging at that time.

At the SE margin, a sharp angular unconformity separates T4 (gently dipping) from the underlying T3 and Upper Cretaceous units (nearly vertical). This unconformity has been clearly observed in field view at the TE-8101 road that leads to Dos Torres de Mercader, where it separates T4 (bedding oriented N63, 20°N) from the La Cañadilla and Órganos de Montoro units (N54, 72°S, and N55 82°S) (Fig. 7a; also see mesostructural information in the next section: site 1, Fig. 8). Such relationship indicates that the highest deformation rate at the SE limb of the synclinorium took place during the T3-T4 transition. Although without such clear evidence, the same seems to occur at the NW limb.

In the NW margin, the units T3, T4 and T5 crop out and present clear unconformities in between (Fig. 7b). An angular unconformity separates T3 and T4, with T3 lying in a sub-vertical position whilst T4 dips 50° SE (Fig. 7b). The relationship between T4 and T5 appears as a conspicuous syntectonic unconformity (Fig. 7c): the dip of bedding is about 50° SE in the oldest T4 layers and becomes gentler upwards up to become nearly horizontal in T5. This suggests that the development of the NW limb would have finished later than the SE limb, by the T4-T5 transition.

The present-day southern basin margin is controlled by an E-W trending, northwards verging anticline. This fold clearly deforms T2 and T3, which are nearly vertical at its northern, steep limb. No relationship of T4 or T5 with this anticline can be observed. Nevertheless, T5 (perhaps also T4) unconformably overlies the Cretaceous units at the southern, gentle limb, T2 and T3 being absent. This suggests that the area south of the CC basin was uplifted, preventing sedimentation (or inducing erosion) of T2 and T3 prior to T5 (maybe also prior to T4). The base of T5 lies at a similar altitude (about 1000 m a.s.l.) south and north

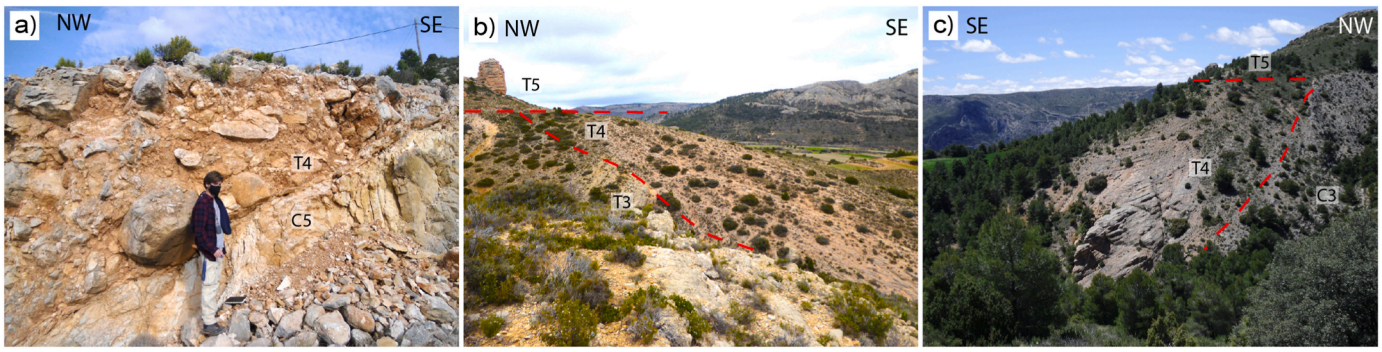

Fig. 7. a) Angular unconformity between the T4 unit and the Órganos de Montoro Formation (C5). The erosive surface was subsequently reactivated as a reverse fault (see structural orientations in stereoplots 1L, 1FC and 1FT of Fig. 8). (b) Unconformities between T3, T4 and T5 units in the NW limb of the CC syncline. c) Syntectonic unconformity between T4 and T5 units at the NW limb of the CC syncline.

of the synclinorium; such nearly horizontal attitude suggests that no significant deformation has affected this unit on a macrostructural scale.

7. Mesostructures and paleostress analysis

Mesostructural data collected in selected outcrops of several Cenozoic units allow us to approach the paleostress conditions under which the macrostructures developed. Five data sites have provided reliable paleostress results that can be confronted, and reasonably correlated, with the regional paleostress framework. The data sources are striated fault planes and pressure-solution lineations in conglomerate pebbles. The results are compiled in Fig. 8.

Site 1 is a complex outcrop in which the unconformity between T4 conglomerates and Upper Cretaceous limestones is exposed. Both units have been surveyed, obtaining several samples of pressure-solution lineations and fault-slip data that have been submitted to different stress inversion techniques. The orientations of pressure-solution lineations in conglomerates provide two distinct, nearly horizontal σ_1 axes with azimuts 163 and 052 (Fig. 8, stereoplot 1L. Although a small subgroup of lineations trend NW-SE, it is interpreted as a deviation of the main, NNW-SSE cluster. Stylolithic peaks in Cretaceous limestones provide a single solution (σ_1 157; Figs. 8 and 1L). Striated faults in both units have provided stress tensors very close to each other, with σ_1 directions 164 and 172, respectively, and nearly vertical σ_3 axes (Fig. 8, 1FC and 1FT). In summary, four out of five individual σ_1 axes are oriented NNW-SSE and were recorded after folding of the T4 unit (they are consistently horizontal in spite of the steep bedding dip); other σ_1 axes (ESE-WSW and NE-SW) are less represented.

Site 2 (T4 conglomerates) shows a vast majority of subhorizontal solution lineations (Fig. 8c) clustered around N145°E (subsequent to folding of T4 unit) and a few ones oriented NNE-SSW (Figs. 8 and 2L). In the same outcrop, a conspicuous reverse fault zone shows abundant striated fault planes (Fig. 8d). The homogeneous orientation of both planes and slickenlines (Figs. 8 and 2F) does not permit to obtain significant paleostress results, but only a nearly pure reverse kinematics of the fault zone that is consistent with a compression direction within the SE quadrant.

In site 3 (T3 conglomerates), most solution lineations have azimuths clustered around N120°E, but some of them are close to horizontal while others show high plunges and are nearly parallel to bedding (Figs. 8 and 3L). They can be interpreted as a result of a horizontal, ESE-WNW trending compression that was active before and after folding of the T3 unit). Some scarce lineations are oriented NE-SW.

Site 4 (T3 conglomerates) show three lineation clusters (Figs. 8 and 4L) representing the three main regional compression directions (113, 170, 057). Based on cross-cut relationships observed in three different pebbles, it was possible to locally define the chronological order between lineations clustered around N113°E (earlier) and those around N57°N (younger).

8. Interpretation and evolutionary model

The interpretation that follows is based on the following results: (i) Jurassic, Cretaceous and Cenozoic units were mapped in the studied area: the Jurassic, with an approximately constant thickness; the Cretaceous, with a decrease in thickness towards the North; the Cenozoic occupying the core of the CC syncline. (ii) Six unconformities were identified, out of which two connected with an extensional period (J5-C1, C1–C2), and other four linked with an orogenic period (C7-T2, T2-T3, T3-T4 and T4-T5). (iii) Three sets of contractive structures were identified (NE-SW, E-W, N–S, in order of importance). (iv) The tectono-sedimentary relationships can be inferred from to the onlap geometry of the T2 and T3 units to the South, and the angular unconformities between the T3, T4 and T5 units to the North. (v) Striated fault planes and pressure-solution lineations in conglomerate pebbles, indicate the existence of four different paleostress directions connected to different tectonic episodes.

The CC syncline belongs to the Linking Zone of the NE Iberian Chain, where most of the contractive structures have a NE-SW to E-W trend that differs from the overall NW-SE trend of the chain. Many of those structures represent the positive inversion of previous extensional faults, the latter being responsible for thickness variations of the Lower Cretaceous units and their angular unconformity with the Upper Cretaceous Mosqueruela Fm. in the study area. When analysed in detail, it is possible to infer that such tectonic inversion took place under the influence of different compression directions, in combination with spatial heterogeneity of the stress-strain fields due to stress deflection and strain partitioning processes. All of them can explain the variety of resulting structures.

The CC syncline is controlled by a double, NE-SW striking thrust system in its NW margin. Based on the cross sections previously presented (Fig. 4), it is possible to infer how this double thrust was formed. The most probable sequence would be the upper thrust being the first to be formed, originally as a normal fault that was subsequently reactivated as a reverse fault, originating the hanging-wall anticline and a footwall syncline. The lower thrust formed during a subsequent deformation stage (in normal footwall sequence), cutting across the footwall syncline. After this, the deformation continued, developing the above-mentioned structures, tightening the folds, which also resulted in steepening of thrusts up to a close-to-vertical position. To the SE, the inversion of a blind fault, involving the basement and inherited from the Cretaceous extension, gave rise to a thrust, elevating the SE border of the CC basin.

This structural evolution took place under the action of several compressional stress fields, which should be considered in order to build a valid evolutionary (kinematical, dynamical and tectono-sedimentary)

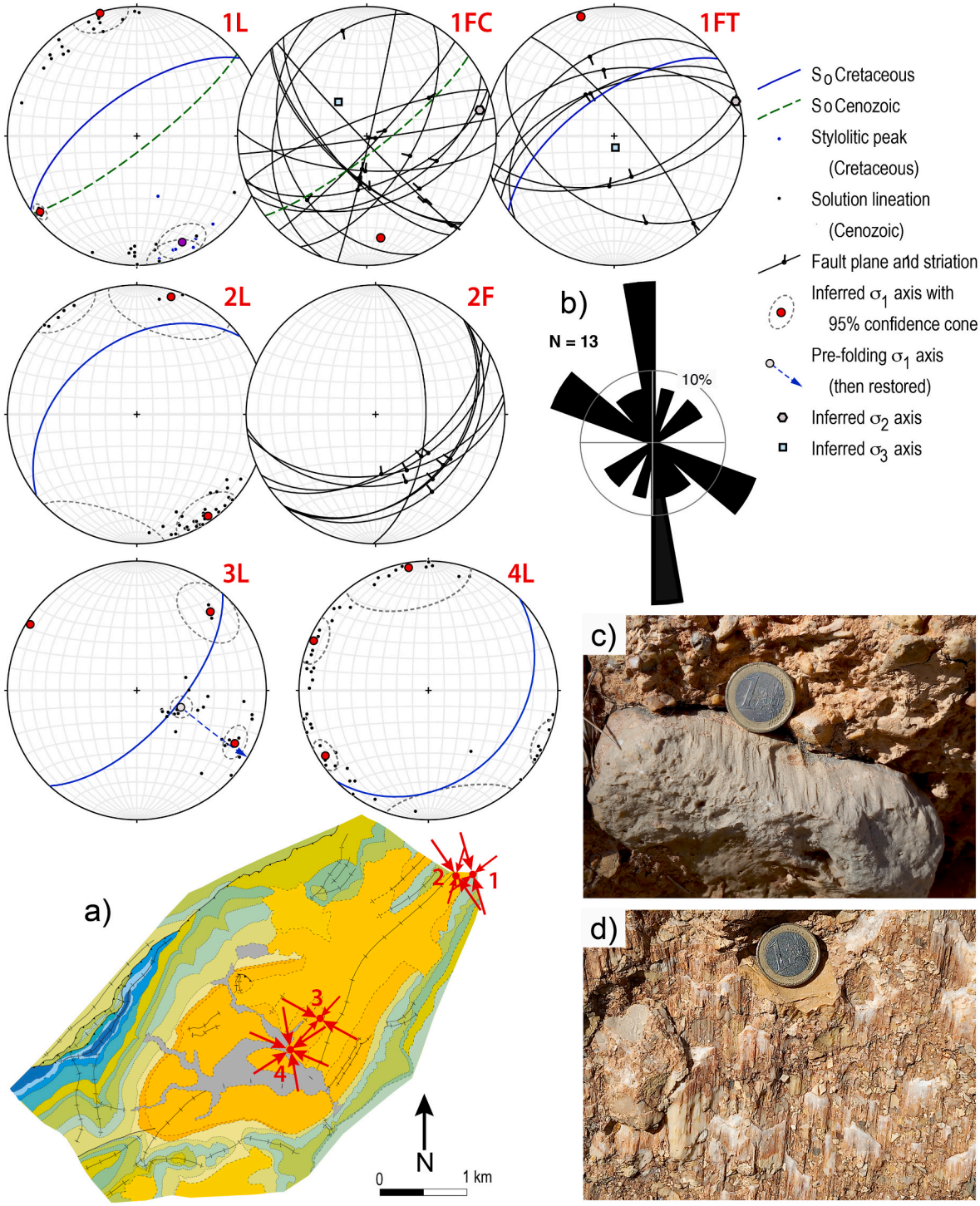

Fig. 8. Mesostructures at outcrop scale and paleostress analysis. 1L, 2L, 3L and 4L: Solution lineations in conglomerate pebbles of sites 1, 2, 3 and 4, respectively. 1FC and 1FT: fault data from Cretaceous and Cenozoic materials, respectively, in site 1. 2F: fault data from Cenozoic materials in site 2. (a) Location map of the data sites. (b) Synthetic rose diagram of directions of the inferred compression axes (σ_1). (c) Example of limestone pebble with solution lineations in site 2. d) Example of striated reverse fault surface in site 2.

model. The local σ_1 directions recorded in the CC area can be closely correlated with the regional paleostress evolution proposed by Liesa and Simón (2007, 2009) and Simón (2006a, 2019b). Fig. 8b shows the distribution of the 13 individual directions, with three clear maxima: N–S, ESE-WNW and NE-SW (in order of importance). The directions around N–S (NNW-SSE to NNE-SSW indeed), profusely and consistently recorded, clearly postdate the folds that affect T4 in sites 1, 2 and 4 (i.e., post-Oligocene). It should be attributed to the Late Betic compressional stage (Early Miocene). The WNW-ESE directions, overall coeval of NE-SW trending folds postdating T3 in site 3, and also fairly represented in site 4, should be attributed to the Early Betic stage (Eocene-Early Oligocene). The minority NE-SW direction, consistently younger than the WNW-ESE one in site 4, can be attributed to the Iberian compression (Oligocene). Finally, the minority NNE-SSW lineations in site 2 could be tentatively assigned to the Late Pyrenean compressional stage (Early Miocene).

The main tectono-sedimentary relationships observed at the margins of CC basin can be summarized and interpreted as follows.

(i) Onlap relationship between T2+T3 and Mesozoic units in both limbs, together with eastwards sourcing of T2 materials, evidence an earlier onset of the synclinorium during deposition of T2. The sharp unconformity separating T3 from T4 (see Fig. 7a and b) indicates that the highest deformation rate took place during the T3-T4 transition. In summary: if the Cenozoic units of our basin are assumed to be approximately coeval of their correlative ones in the Aliaga and Montalbán basin, the overall CC synclinorium mostly developed during late Eocene to early Oligocene times.

(ii) The syntectonic unconformity between T4 and T5 (see Fig. 7c) indicates that the development of the NW limb was further prolonged up to the T4-T5 transition, at the end of the Oligocene. This transition coincides with the stage at which the final structure of the Linking Zone is configured (Guimerà, 1988; González and Pérez, 2018).

(iii) The absence of the T2 and T3 (see map in Fig. 3 and cross-sections in Fig. 4a and c) units in the area south of the CC basin suggests that this was uplifted prior to T5 deposition and, perhaps, also prior to T4. Concerning T3, it is difficult to admit that its entire thickness (almost 500 m) could have existed, then removed, at this southern area. Therefore, a southern basin margin, probably controlled by an E-W trending monocline developed above a basement fault, should be considered at least during sedimentation of T3. Since the base of T5 lies at a similar altitude south and north of the syncline, we infer that such structural setting had finished operating prior to sedimentation of T5.

It should be noted that the present-day E-W trending fold does not need to be the structure that determined the southern margin of CC basin. The T5 unit does not rest unconformably on the fold, and so this contractive structure could result from a later orogenic episode, active in the whole region during the Early Miocene (Late Betic and Late Pyrenean compressions, whose maximum stress axes trend NNW-SSE and NNE-SSW, respectively; Liesa and Simón, 2009). Under such favourable compressional stress fields, the E-W trending fold could nucleate on the previous monocline/basement fault, that controlled the southern boundary of the basin. Numerous E-W to ENE-WSW trending folds, locally superposed to the previous Paleogene folds (Simón, 2004, 2005), developed during this tectonic episode throughout the northern Maestrazgo region.

Considering the ensemble of macrostructural, tectono-sedimentary and paleostress results obtained in the CC area, and having in mind the regional tectonic framework, the following evolutionary model is proposed (Fig. 9).

(1) During the sedimentation of T2 (Early-Middle Eocene), under the Early Betic compression (trending N110°E to N130°E), the Ladruñán anticline and the CC syncline began to form. The steep limb shared by both folds was probably nucleated on a previous NE-SW striking fault, which had been an extensional fault during the Early Cretaceous and was subsequently inverted under the Eocene compression. The NW limb also began to rise, probably controlled by a second inherited fault, so that the syncline worked as a foreland basin of the SE thrust and a piggy-back basin with respect to the NW one. Both hypothetical faults or fault zones are parallel to each other and show a right relay arrangement. During the T2 stage, the CC basin is one of the small basins that are individualized, and in which sedimentation becomes confined. Before, during the sedimentation of T1 (Paleocene-early Eocene?), the transition area from the Iberian Chain to the Ebro Basin had constituted a single fluvial-alluvial basin fed from the south (González and Pérez, 2018).

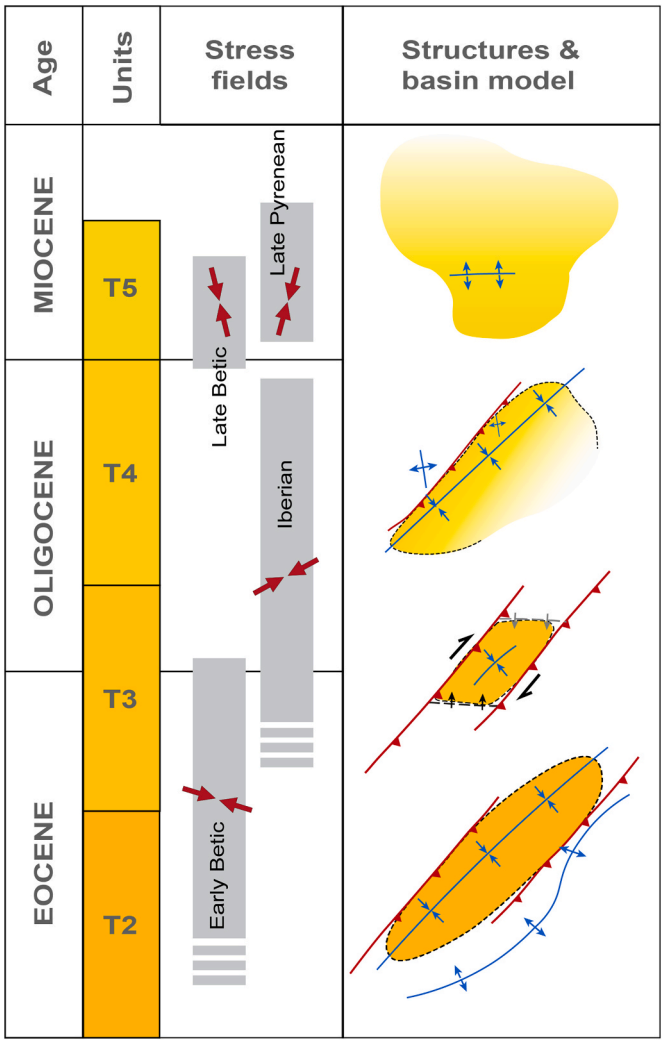

Fig. 9. Evolutionary model of the Cuevas de Cañart basin. See explanation in the text.

(2) During the sedimentation of T3 (Late Eocene-Early Oligocene) the Early Betic compression remained active, but the evolution of other Cenozoic basins (Montalbán, Aliaga) also suggests the onset, by that time, of the Iberian compression (N040°E to N080°E). The latter also continued during the deposition of the T4 unit (Middle-Late Oligocene). Under such oblique compressions, the NE-SW striking inherited fault zones could work as transpressional structures. More precisely, compression along either N110°E (Early Betic) or N070-080°E (Iberian) directions was able to move those faults with a dextral component. This would make the relay zone to act as an extensional one, allowing the previous syncline to become, episodically, a pull-apart basin. This represents a further step in the progressive individualization of the basin, and could explain the extraordinarily high subsidence and the great thickness (almost 500 m) reached by T3 despite the reduced basin size. Alluvial sedimentation was mainly sourced from the north, which suggests that this sector was isolated from the Ebro basin (González and Pérez, 2018). Nevertheless, also a southern basin margin could exist, controlled by an E-W trending extensional monocline, a subsidiary structure induced by the fault relay kinematics. Besides, the local N–S trending folds in the western corner of the study area, as well as the NW-SE folded thrust described in the NW limb of the main syncline (Fig. 7), would represent primary structures developed

in response to the remote Iberian compression, thus escaping the kinematical constraints imposed by the inherited master faults.

In summary, under compression directions close to E-W, active during the late Eocene and the Oligocene, distinctly oriented structures developed more or less coevally: transpressional NE-SW faults; small contractive, N–S to NW-SE trending structures; and a secondary E-W trending extensional monocline. The CC basin would have evolved during most of the Eocene and Oligocene periods responding to a mixed, syncline/piggy-back + pull-apart model.

(3) Such a structural setting had ceased operating when T5 was deposited, by the beginning of the Miocene, a time when sedimentation expanded again beyond the margins of the small Palaeogene basins. The E-W trending anticline at the southern border of the CC basin is, probably, the only structure developed after T5, nucleated on the previous extensional monocline and coeval to other parallel contractional structures developed throughout the northern Maestrazgo (Simón, 2004). All of them respond to the last orogenic episodes of the Iberian Chain: Late Betic (NNW-SSE) and Late Pyrenean (NNE-SSW) compressions.

9. Discussion

9.1. Fold systems and tectonic episodes

The Iberian Chain, despite its overall NW-SE trend, shows a variety of structural directions, with sectors where NW-SE folds and thrusts predominate (mostly the Castilian branch) and others where E-W and NE-SW structures prevail (mostly the northern Maestrazgo sector). The CC area belongs to the latter ones; more precisely, it is framed within the sinuous fold-and-thrust belt that makes the Linking Zone with the Catalonian Ranges.

To explain the tectonic evolution of the Iberian Chain by combining such structural diversity and its complex dynamic framework within the Iberian plate, is not an easy task. Very different, even antagonistic, models have been proposed. Guimerà (1988) proposed that the entire structural development of the Iberian Chain, Catalonian Ranges and their intermediate Linking Zone can be explained by an only contractional process with the maximum compression oriented N010°E. This would have activated inherited faults with two prevalent directions: NW-SE, in a dextral transpressional regime (Iberian Chain s.s.), and NE-SW, sinistral (Linking Zone and Catalonian Ranges). Also De Vicente et al. (2009) state that the macrostructure of the Castilian (western) Branch of the Iberian Chain can be explained by a single N–S shortening under a constrictive deformation regime, which induced transpression and strain partitioning along the main NW-SE trending inherited faults. These models focus on the spatial heterogeneity of the deformation, while considering a linear dynamic evolution. In contrast, other models emphasised the temporal heterogeneity, i.e. the existence of tectonic phases with different compression directions due to the changing geodynamic framework (e.g. Simón, 1982; Jabaloy et al., 2002). More recently, Liesa and Simón (2009), based on an extremely large paleostress database, have demonstrated that (i) a single stress field with multiple perturbations cannot explain the ensemble of compression directions recorded in the Iberian Chain, but also that (ii) structures exhibiting distinct directions should not necessarily be the product of different compression episodes. In summary, a realistic tectonic model for the region should include both temporal and spatial stress heterogeneity (including successive remote compression directions, stress perturbations, stress and strain partitioning …), and hence both temporal and spatial changes in faulting regimes (Simón et al., 2008; De Vicente et al., 2009; Liesa and Simón, 2009).

The coexistence of several fold sets in a small area such as the CC basin should be interpreted within such tectonic framework. Their orientations are strongly conditioned by the presence of previous basement faults inherited from Variscan and Mesozoic times, but their activation is a consequence of the stress field prevailing in each episode. The main NE-SW trending folds and faults could develop since very early Cenozoic times under ESE-WSW to SE- NW trending compression (Early Betic compressional episode, as defined by Liesa and Simón, 2009). They were able to continue during later stages of the Iberian compression (ENE-WSW), while in other sectors of the chain NW-SE folds and faults dominated. Finally, the E-W trending fold that makes the southern margin of the basin, superposed to the NE-SW trending syncline (Simón, 2004), probably resulted from the Late NNW-SSE to NNE-SSW compressional stress episodes (Late Betic and Late Pyrenean compressions, respectively; Liesa and Simón, 2009).

9.2. Basin model

The proposed evolutionary model (Fig. 9) states the CC Cenozoic basin developed during most of the Eocene and Oligocene, sharing characteristics of two end-member basin models: piggyback/foreland and pull-apart basin.

The first model, a piggyback basin associated with a previously formed foreland basin, fits well with the style of the Cenozoic internal basins of the Iberian Chain (see Fig. 2), where most NE-SW thrusts consistently verge towards the NW (Canérot et al., 1982). At the NW sector of the study area, there is a NE-SW oriented thrust that could be the one controlling the basin, located in its hanging-wall block. On the other hand, there is also an inferred blind fault at the southern limb of the syncline, for which the basin worked as a foreland basin. In short, it is a synclinal basin sandwiched between thrusts, as commonly found within fold-and-thrust belts where syntectonic sedimentation occurs.

The second model, a pull-apart basin, is strongly suggested by the rhomboidal geometry of the basin in map view. This has a particular interest because the southern limb of the syncline has an impressively straight geometry and is responsible for the separation between the CC syncline and the area occupied by the T5 unit to the south. The two previously mentioned thrusts found both in the northern and southern limbs of the syncline show a consistent right relay arrangement. These might have been subjected to a dextral strike-slip movement at some point in time, after the aforementioned verticalization stage, making the area behave as an extensional relay zone. This could be achieved during the sedimentation of the T3 unit (Late Eocene-Early Oligocene), under both the Early Betic compression (ESE-WNW) or the Iberian compression (NE-SW to ENE-WSW). Subsequent activation of the southern border under the Late Pyrenean compression, giving rise to the prominent E-W fold, enhanced the rhomboidal contour of the basin and made the relay zone to switch to a compressional one.

The proposed model is a combination of the two aforementioned ones. However, even though transpressive tectonic evidence has been found within the Iberian Chain, no pull-apart Cenozoic basin has yet been described outside of the Castilian Branch. The piggy-back model is more commonly found within the Iberian context but, by itself, cannot explain the massive localized Cenozoic subsidence at the CC syncline (500 m in thickness in its core). We have shown how the structural evolution of the area followed different stages characterized by both strike-slip and compressive tectonic regimes. Therefore, the basin evolution could be described as a stage by stage, piggy-back to pull-apart and back, model.

We should admit that our direct field observations concerning the kinematics of the map-scale faults only evidence nearly pure reverse slip on them (e.g., mesostructural data represented in stereoplots 1FC, 1FT, 2F of Fig. 7). No evidence on strike-slip or normal slip was acquired during field survey along the fault traces, which means that our proposed basin model has only a hypothetical status. Nevertheless, the notion of a significant strike-slip component in both basement and cover structures of the Iberian Chain has been broadly documented from map and outcrop data. In particular, the strong bend exhibited by folds and thrusts along the Ejulve-Alcorisa-Castellote area (see Fig. 1a)

constitutes, according to Simón (1981) and Guimerà (1984, 1988), an evidence of sinistral slip on a major, NE-SW striking basement fault. Although such basement strike-slip faults might have remained as blind faults during alpine compression, their control over syntectonic basins in the cover could have been equally effective. Concerning the hypothetic dextral movement on NE-SW striking faults, invoked for the pull-apart basin model, we recognize that it is less reliably established. Such slip regime is just deduced from the assumption that such faults moved under either ESE-WNW or ENE-WSW trending remote compression (inferred from regional and local paleostress analysis).

9.3. Overall view within the near and far regional framework

The CC basin evolved within a compressional context, as other numerous Cenozoic basins in the northeastern Iberin Chain. The Aliaga and Montalbán basins are the most intensely studied from both the structural and the tectono-sedimentary point of view.

The Aliaga basin is a piggy-back basin associated with the N-verging Utrillas thrust. During the Eocene-Early Miocene, its displacement was approximately 5–8 km (González and Guimerà, 1993; Casas et al., 2000), with successive ENE, NNE and N transport directions (Simón and Liesa, 2011). The basin is a complex syncline whose septentrional limit is bounded by a footwall accommodation monocline, and its meridional limit is defined by a set of WSW-ENE structures associated with the Cobatillas thrust (González and Guimerà, 1993). The structure of the Aliaga basin is entirely linked to the Alpine compression, including two sets of folding structures that bound the basin and also represent internal deformation of its sedimentary units. The first set trends N–S to NW-SE, while the second one shows an ENE-WSW direction. These two sets produced some spectacular superposition structures (Simón, 2004, 2005) that indicate that the ENE-WSW folds are younger than the NW-SE to N–S set. According to Simón (2006a), this basin went through four main compressional episodes, consistent with the evolutionary model of stress fields proposed by Liesa and Simón (2009) for the overall Iberian Chain.

- ESE-WNW, affecting up to T3 (*Early Betic* compression; Eocene-Early Oligocene).
- ENE-WSW, affecting up to T4 (*Iberian* compression; Oligocene).
- SSE-NNW, affecting up to T5 (*Late Betic* compression; Oligocene-Miocene transition)
- NNE-SSW, affecting up to T5-T6 *(Late Pyrenean* compression; Early-Middle Miocene).

The Montalbán basin is located within the Aragonese branch of the Iberian Chain, as a southeastern prolongation of the Neogene Calatayud Basin. It is bounded to the North by the Paleozoic-cored Montalbán anticline, and to the South by the Utrillas thrust. Its core is occupied by six tectono-sedimentary units that together have over 2000 m in thickness (Pérez et al., 1983; Pérez, 1990; Casas et al., 2000). This allows a direct correlation with the Aliaga units (Pardo et al., 1989), also because both basins evolved associated to the Utrillas thrust. However, whilst Aliaga is a piggy-back basin, the Montalbán basin is a foreland basin in relation to this structure. According to Simón (2019b), the Montalbán basin went through the exact same evolutionary stages as the Aliaga basin, described above, undergoing the same sequence of compression episodes: ESE-WNW, NE-SW, NNW-SSE and NNE-SSW.

Similar structural and evolutionary complexity is found in the Zaorejas basin (Guadalajara province, western Iberian Chain; Rodríguez-Pascua and De Vicente, 1998). This is a trapezoidal-shaped syncline structure, developed as the local foreland basin of a E-W to ENE-WSW trending, S verging fold belt. Laterally, it is framed by two NNW-SSE fault zones with associated box folds, exhibiting positive flower style and revealing a dextral transpressional slip regime. In addition, a N–S large sinistral transcurrent fault cuts across the southeastern block of the basin. Two main tectonic episodes are interpreted by Rodríguez-Pascua and De Vicente (1998) on the basis of macro- and mesostructural analysis, and tectono-sedimentary relationships: (i) NNW-SSE compression, active during Eocene-Oligocene times, which gave rise to the ENE-WSW trending folds and a wide progressive unconformity at the northern basin margin; it would be compatible with sinistral slip on the N–S fault. (ii) N–S to NNE-SSW compression, active during the Early Miocene, which tightened the northern folds and activated the sinistral strike-slip faults. Within the regional stress framework, those episodes could be assimilated to the Early Betic and Late Betic-Late Pyrenean compressions, respectively, although the possibility of spatial perturbation of compression directions close to the NW-SE dextral faults should also be considered in this area (Liesa and Simón, 2009).

Briefly, distinct intra-mountain basins developed during the Alpine compression in the Iberian Chain show similar evolutionary patterns, despite their particular structural directions imposed by the tectonic inheritance. In all cases, such evolution was not linear, but made of successive tectonic episodes under the strongly heterogeneous Cenozoic compressional stress fields.

Some similarities arise when comparing the CC syncline with compressional and/or strike-slip features, developed along crustal-scale faults in large-scale basins. As mentioned in the Introduction section, there are examples in different tectonic settings under which rhomb-shaped basins develop: (i) Pure strike-slip settings or transtensional areas (California examples, Sylvester, 1988, the Philippine fault system, Ringenbach et al., 1993, or the Dead Sea, Ben-Avraham et al., 2010); (ii) Basins developed in restraining or compressional jogs and subsequently involved in strike-slip duplexes (cases of the North Anatolian fault, Okay et al., 1999, or the Altyn Tagh fault, Cowgill et al., 2000); (iii) More complex settings in which both spatial and temporal variations are involved, combining features of piggyback or compressional basins, and basins associated with strike-slip during their development, such as the case of the Falcon basin, in northern Venezuela (Audemard, 1995; Baquero et al., 2015), the Pannonian basin (Fodor et al., 1999), or the Xunhua basin (Liu et al., 2013).

Salt tectonics also provide an interesting view in the development of rhomb-shaped basins, linked or not with strike-slip tectonics (Smit et al., 2008; Teixell et al., 2017). In the Iberian Chain, recent interpretations promote or restrain, alternatively, the influence of diapirism in basin formation during the Mesozoic (see, e.g. Vergés et al., 2020; Liesa et al., 2023). In the case of the CC syncline, the salt levels probably conditioned the basement-cover relationships in the extensional stage, similarly to other sectors of the chain (Liesa et al., 2018 and references therein). Neither the superposition of thrust sheets within the thin-skin scenario, nor its verticalization seem to leave much space for the development of (subsequently squeezed?) diapirs at the basin borders during the Cenozoic.

The process of fault segmentation along strike-slip faults, provides different structural directions (Aydin and Nur, 1985; de Joussineau and Aydin, 2009) and folding trends, as occurring in the CC syncline. In these cases, a strong transfer of deformation from the basement to the cover is necessary to generate accomodation space and hence a significant thickness for the sedimentary filling. Combined mechanisms (i.e. strike-slip and compression) at zones of fault interference within compressional settings, with or without a significant transport in a piggyback style (Sun et al., 2006; Liu et al., 2007, 2013; Zhou and Schoenbohm, 2015), provide a more efficient way for generating both subsidence zones and source areas for the sedimentary filling of the basin (in the case of the CC syncline, the Cenozoic materials cropping out at the core of the structure). The existence of basement anisotropies of different directions, that seems to be a fair interpretation for the CC syncline, also provides an explanation for the different structural trends, either in basement or cover rocks (Morozov et al., 2014).

Finally, an interesting issue also arises when we consider the orientation of stress axes during basin evolution (the interpretation proposed in this work for the origin of the CC basin). When the different

compressional stress directions, during basin history, approach the directions of faults, or perpendicular to fault planes, the probability of having different types of displacement (i.e., switching from right lateral to left-lateral movement or component) also increases (see, e.g. Decker, 1996; Decker et al., 2005). These kinds of structures fit well with the structures found in the CC syncline and provide a key for interpreting other basins. This factor increases when faults of different scales interact between them in a lithospheric to crustal scale (Fodor et al., 1999), because of stress perturbations in the vicinity of large faults, even though these are below the surface (Casas-Sainz and Maestro-González, 1996).

10. Conclusions

The NE-SW trending Cuevas de Cañart (CC) syncline basin developed under the Paleogene compression, associated to parallel thrusts that represent the positive inversion of Cretaceous extensional faults. Its NW limb is controlled by a double thrust probably developed in a footwall sequence, their surfaces reaching an almost vertical position.

The coexistence of distinctly oriented fold sets in the CC basin results from both the structural inheritance (basement Variscan and Mesozoic faults) and the succession of different compressional stress fields, recorded as local σ_1 directions that can be closely correlated with the regional paleostress framework. The ensemble of macrostructural, tectono-sedimentary and paleostress results indicate that the CC basin evolved during most of the Eocene and Oligocene periods responding to a mixed, syncline/piggy-back + pull-apart model. The following evolutionary episodes can be distinguished.

1) Beginning of development of the Ladruñán anticline and the CC syncline under the Early Betic compression (N110°E to N130°E; Eocene in age). Both the steep limb shared by both folds and the NW limb of the CC syncline were probably controlled by inherited, Early Cretaceous NE-SW extensional faults. The syncline worked as a foreland basin of the SE thrust and a piggy-back basin with respect to the NW one.
2) Between Late Eocene and Late Oligocene times, both bounding, right-relay arranged faults could work as transpressional structures with a dextral component under both the Early Betic (N110°E) and the Iberian (N070-080°E) oblique compressions. The relay zone acted as an extensional one, allowing the previous syncline to become a pull-apart, highly subsident basin during sedimentation of T3 unit.
3) By the beginning of the Miocene, under the last compressional episodes of the Iberian Chain (Late Betic, NNW-SSE; Late Pyrenean, NNE-SSW), the E-W trending anticline developed at the southern basin margin, nucleated on a previous extensional monocline induced by the fault relay kinematics.

CRediT authorship contribution statement

Lourenço Steel Hart: Conceptualization, Methodology, Validation, Formal analysis, Investigation, Data curation, Writing – original draft, Writing – review & editing, Visualization, Project administration. **Antonio M. Casas-Sainz:** Conceptualization, Methodology, Validation, Formal analysis, Investigation, Resources, Writing – review & editing, Visualization, Supervision. **José L. Simón:** Conceptualization, Methodology, Validation, Formal analysis, Investigation, Resources, Writing – review & editing, Visualization, Supervision.

Declaration of competing interest

The authors declare that they have no known competing financial interests or personal relationships that could have appeared to influence the work reported in this paper.

Data availability

Data will be made available on request.

Acknowledgements

We are very grateful to Marcos Aurell, Carlos Liesa and Ana Simón for their help with field work and suggestions to the basin model, as well as to Gerardo de Vicente, another anonymous reviewer, and the editor for their helpfull suggestions. This work was partly supported by the Agencia Estatal de Investigación (AEI/10.13039/501100011033) of the Spanish Government (projects PID2019-108753 GB-C22 and PID2019-108705 GB-I00), and the Gobierno de Aragón (Geotransfer Research Group, E32-20R).

References

Allen, P.A., Allen, J.R., 2013. Basin Analysis: Principles and Application to Petroleum Play Assessment. John Wiley & Sons, New York.
Allmendinger, R.W., Cardozo, N., Fisher, D.M., 2011. Structural Geology Algorithms: Vectors and Tensors. Cambridge University Press, Cambridge.
Álvaro, M., Capote, R., Vegas, R., 1979. Un modelo de evolución geotectónica para la Cadena Celtibérica. Acta Geológica Hispánica, Libro Homenaje Prof. Solé Sabaris 14, 174–177.
Angelier, J., Mechler, P., 1977. Sur une méthode graphique de recherche des contraintes principales également utilisables en tectonique et en séismologie: la méthode des dièdres droits. Bull. Soc. Geol. Fr. 7, 1309–1318.
Antolín-Tomás, B., Liesa, C.L., Casas, A., Gil-Peña, I., 2007. Geometry of fracturing linked to extension and basin formation in the Maestrazgo basin (Eastern Iberian Chain, Spain). Rev. Soc. Geol. Espana 20, 351–365.
Aurell, M., Bádenas, B., Canudo, J.I., Castanera, D., García-Penas, A., Gasca, J.M., Martín-Closas, C., Moliner, L., Moreno-Azanza, M., Rosales, I., Santas, L., Sequero, C., Val, J., 2019. Kimmeridgian–berriasian stratigraphy and sedimentary evolution of the central Iberian rift system (NE Spain). Cretac. Res. 103, 104153.
Aydin, A., Nur, A., 1982. Evolution of pull-apart basins and their scale independence. Tectonics 1, 91–105.
Aydin, A., Nur, A., 1985. The types and role of stepovers in strike slip tectonics. In: Biddle, K.T., Christie-Blick, N. (Eds.), Strike-slip Tectonics and Sedimentation, vol. 37. Society of Economic Paleontologists and Mineralogists Special Publication, pp. 35–44.
Baquero, M., Acosta, J., Kassabji, E., Zamora, J., Sousa, J.C., Rodríguez, J., Schneider, F., 2009. Polyphase development of the Falcón Basin in northwestern Venezuela: implications for oil generation. Geological Society, London, Special Publication 328 (1), 587–612.
Baquero, M., Grande, S., Urbani, F., Cordani, U., Hall, C., Armstrong, R., 2015. In: Bartolini, C., Mann, P. (Eds.), Petroleum Geology and Potential of the Colombian Caribbean Margin, 108. AAPG Memoir, pp. 105–138.
Basile, C., Brun, J.P., 1999. Transtensional faulting patterns ranging from pull-apart basins to transform continental margins: an experimental investigation. J. Struct. Geol. 21, 23–37.
Ben-Avraham, Z., Lyakhovsky, V., Schubert, G., 2010. Drop-down formation of deep basins along the Dead Sea and other strike-slip fault systems. Geophy. J. Int. 181 (1), 185–197.
Biddle, K.T., Christie-Blick, N., 1985. In: Biddle, K.T., Christie-Blick, N. (Eds.), Strike-slip Tectonics and Sedimentation. Society of Economic Paleontologists and Mineralogists Special, 37. Publication, pp. 376–386.
Canérot, J., Cugny, P., Pardo, G., Salas, R., Villena, J., 1982. Ibérica central-maestrazgo. In: El Cretácico de España. Universidad Complutense de Madrid, pp. 273–344.
Capote, R., Muñoz, J.A., Simón, J.L., Liesa, C.L., Arlegui, L.E., 2002. Alpine tectonics I: the alpine system north of the betic Cordillera. In: Gibbons, W., Moreno, T. (Eds.), The Geology of Spain. The Geological Society, London, pp. 367–400.
Cardozo, N., Allmendinger, R.W., 2013. Spherical projections with OSXStereonet. Comput. Geosci. 51, 193–205.
Casas, A.M., Casas, A., Pérez, A., Tena, S., Barrier, L., Gapais, D., Nalpas, T., 2000. Syntectonic sedimentation and thrust-and-fold kinematics at the intra-mountain Montalbán Basin (northern Iberian Chain, Spain). Geodin. Acta 13, 1–17.
Casas-Sainz, A., Faccenna, C., 2001. Tertiary compressional deformation of the Iberian plate. Terra Nova 13 (4), 281–288.
Casas-Sainz, A.M., Maestro-González, A., 1996. Deflection of a compressional stress field by large-scale basement faults. A case study from the Tertiary Almazán basin (Spain). Tectonophysics 255, 135–156.
Cheng, F., Jolivet, M., Guo, Z., Wang, L., Zhang, C., Li, X., 2021. Cenozoic evolution of the Qaidam basin and implications for the growth of the northern Tibetan plateau: a review. Earth-Sci. Rev. 220, 103730.
Cobbold, P.R., Davy, P., Gapais, D., Rossello, E.A., Sadybakasov, E., Thomas, J.C., Tondji Biyo, J.J., de Urreiztieta, M., 1993. Sedimentary basins and crustal thickening. Sediment. Geol. 86, 77–89.
Cowgill, E., Yin, A., Feng, W.X., Qing, Z., 2000. Is the North Altyn fault part of a strike-slip duplex along the Altyn Tagh fault system? Geology 28 (3), 255–258.
Cunningham, W.D., Mann, P., 2007. Tectonics of Strike-Slip Restraining and Releasing Bends, vol. 290. Geological Society, London, Special Publication, pp. 1–12.

de Joussineau, G., Aydin, A., 2009. Segmentation along strike-slip faults revisited. Pure Appl. Geophys. 166, 1575–1594.
De Vicente, G., Muñoz-Martín, A., 2013. The Madrid Basin and the Central System: a tectonostratigraphic analysis from 2D seismic lines. Tectonophysics 602, 259–285.
De Vicente, G., Vegas, R., Martín, A.M., Silva, P.G., Andriessen, P., Cloetingh, S., González-Casado, J.M., Van Wees, J.D., Álvarez, J., Carbó, A., Olaiz, A., 2007. Cenozoic thick-skinned deformation and topography evolution of the Spanish Central System. Global Planet. Change 58, 335–381.
De Vicente, G., Vegas, R., Muñoz-Martín, A., Van Wees, J.D., Casas-Sáinz, A., Sopeña, A., Sánchez-Moya, Y., Arche, A., López-Gómez, J., Olaiz, A., Fernández-Lozano, J., 2009. Oblique strain partitioning and transpression on an inverted rift: the Castilian Branch of the Iberian Chain. Tectonophysics 470, 224–242.
De Vicente, G., Cunha, P.P., Muñoz-Martín, A., Cloetingh, S., Olaiz, A., Vegas, R., 2018. The Spanish-Portuguese Central System: an example of intense intraplate deformation and strain partitioning. Tectonics 37, 4444–4469.
Decker, K., 1996. Miocene tectonics at the Alpine-Carpathian junction. Mitt. Ges. Geol. Bergbaustud. Osterr. 41, 33–44.
Decker, K., Peresson, H., Hinsch, R., 2005. Active tectonics and Quaternary basin formation along the Vienna Basin Transform fault. Quat. Sci. Rev. 24, 305–320.
Einsele, G., 2000. Sedimentary Basins: Evolution, Facies, and Sediment Budget. Springer, Berlin.
Etchecopar, A., Vasseur, G., Daignieres, M., 1981. An inverse problem in microtectonics for the determination of stress tensors from fault striation analysis. J. Struct. Geol. 3 (1), 51–65.
Ezquerro, L., 2017. El sector norte de la cuenca neógena de Teruel: tectónica, clima y sedimentación. PhD thesis. Universidad de Zaragoza.
Ezquerro, L., Luzón, A., Simón, J.L., Liesa, C.L., 2019. Alluvial sedimentation and tectono-stratigraphic evolution in a narrow extensional zigzag basin margin (northern Teruel Basin, Spain). J. Palaeogeogr. 8, 1–25.
Fodor, L., Csontos, L., Bada, G., Györfi, I., Benkovics, L., 1999. Tertiary Tectonic Evolution of the Pannonian Basin System and Neighbouring Orogens: a New Synthesis of Palaeostress Data, vol. 156. Special Publication Geological Society of London, pp. 295–334.
Gómez, J.J., Goy, A., 1979. Las unidades litoestratigráficas del Jurásico Medio y Superior en facies carbonatadas del Sector Levantino de la Cordillera Ibérica. Estudios geol 35, 569–598.
Gómez, J.J., Comas-Rengifo, M.J., Goy, A., 2003. Las unidades litoestratigráficas del Jurásico Inferior de las cordilleras Ibérica y Costeras Catalanas. Rev. Soc. Geol. Espana 16, 227–238.
González, A., 1989. Análisis tectosedimentario del Cenozoico del borde SE de la depresión del Ebro (sector bajoaragonés) y cubetas ibéricas marginales. PhD thesis. Universidad de Zaragoza.
González, A., Guimerà, J., 1993. Sedimentación sintectónica en una cuenca transportada sobre una lámina de cabalgamiento: la cubeta terciaria de Aliaga. Rev. Soc. Geol. Espana 6, 151–165.
González, A., Pérez, A., 2018. El Terciario del sector turolense de la Cuenca del Ebro: una crónica de la estructuración alpina de la Cordillera Ibérica. In: Alcalá, L., Calvo, J.P., Simón, J.L. (Eds.), Geología de Teruel. Instituto de Estudios Turolenses, Teruel, pp. 83–98.
González, A., Pardo, G., Villena, J., Martínez, B., 1985. Análisis tectosedimentario del terciario de Cuevas de Cañart (Prov. de Teruel). Trab. Geol. 15, 169–177.
Guimerà, J., 1984. Palaeogene evolution of deformation in the northeastern Iberian Peninsula. Geol. Mag. 121, 413–420.
Guimerà, J., 1988. Estudi estructural de l'enllaç entre la Serralada Ibèrica i la Serralada Costanera Catalana. PhD Thesis. Universitat de Barcelona.
Hippolyte, J.C., Bergerat, F., Gordon, M.B., Bellier, O., Espurt, N., 2012. Keys and pitfalls in mesoscale fault analysis and paleostress reconstructions, the use of Angelier's methods. Tectonophysics 581, 144–162.
Jabaloy, A., Galindo-Zaldívar, J., González-Lodeiro, F., 2002. Palaeostress evolution of the Iberian Peninsula (Late Carboniferous to present-day). Tectonophysics 357 (1–4), 159–186.
Kaven, J.O., Maerten, F., Pollard, D.D., 2011. Mechanical analysis of fault slip data: implications for paleostress analysis. J. Struct. Geol. 33, 78–91.
Lacombe, O., 2012. Do fault slip data inversions actually yield "paleostresses" that can be compared with contemporary stresses? A critical discussion. Compt. Rendus Geosci. 344, 159–173.
Laville, E., 1988. A multiple releasing and restraining stepover model for the Jurassic strike-slip basin of the Central High Atlas (Morocco). Dev. Geotectonics 22, 499–523.
Li, C., He, D., Sun, Y., He, J., Jiang, Z., 2015. Structural characteristic and origin of intra-continental fold belt in the eastern Sichuan basin, South China Block. J. Asian Earth Sci. 111, 206–221.
Liesa, C.L., 2011. Fracturación extensional cretácica en la sierra del Pobo (Cordillera Ibérica, España). Rev. Soc. Geol. Espana 24, 31–48.
Liesa, C.L., Simón, J.L., 2007. A probabilistic approach for identifying independent remote compressions in an intraplate region: the Iberian Chain (Spain). Math. Geol. 39, 337–348.
Liesa, C.L., Simón, J.L., 2009. Evolution of intraplate stress fields under multiple remote compressions: the case of the Iberian Chain (NE Spain). Tectonophysics 474, 144–159.
Liesa, C.L., Simón, J.L., Casas, A.M., 2018. La tectónica de inversión en una región intraplaca: la Cordillera Ibérica. Rev. Soc. Geol. Espana 6, 151–165.
Liesa, C.L., Casas-Sainz, A.M., Aurell, M., Simón, J.L., Soria, A.R., 2023. Salt tectonics vs. inversion tectonics: the anticlines of the western Maestrazgo revisited (eastern Iberian Chain, Spain). Basin Res. 35, 295–335.
Liu, S., Zhang, G., Heller, P.L., 2007. Cenozoic basin development and its indication of plateau growth in the Xunhua-Guide district. Sci. China Earth Sci. 50 (Suppl. 2), 277–291.
Liu, S., Yang, Y., Deng, B., Zhong, Y., Wen, L., Sun, W., Li, Z., Jansa, L., Li, J., Song, J., Zhang, X., Peng, H., 2021. Tectonic evolution of the Sichuan basin, southwest China. Earth Sci. Rev. 213, 103470.
Liu, S., Zhang, G., Pan, F., Zhang, H., Wang, P., Wang, K., Wang, Y., 2013. Timing of Xunhua and Guide basin development and growth of the northeastern Tibetan Plateau, China. Basin Res. 25 (1), 74–96.
Margarit, O., 2019. Estructura mesozoica y cenozoica del sector Ladruñán-Castellote (Cordillera Ibérica). MSc thesis, Universidad de Zaragoza. https://zaguan.unizar.es/record/86541/files/TAZ-TFM-2019-1474.pdf.
Martín-González, F., Heredia, N., 2011. Complex tectonic and tectonostratigraphic evolution of an Alpine foreland basin: the western Duero Basin and the related Tertiary depressions of the NW Iberian Peninsula. Tectonophysics 502, 75–89.
Morozov, Y.A., Leonov, M.G., Alekseev, D.V., 2014. Pull-apart formation mechanism of Cenozoic basins in the Tien Shan and their transpressional evolution: structural and experimental evidence. Geotectonics 48, 24–53.
Mostafa, M.E., 2005. Iterative direct inversion: an exact complementary solution for inverting fault-slip data to obtain palaeostresses. Comput. Geosci. 31, 1059–1070.
Muessig, K.W., 1984. Structure and Cenozoic tectonics of the Falcón basin, Venezuela, and adjacent areas. Geol. Soc. Am. Mem. 162, 217–230.
Nebot, M., 2016. Mesozoic Extension and Cenozoic Contraction in the Eastern Iberian Chain (Maestrat Basin). PhD Thesis. Universitat de Barcelona. www.tdx.cat/bitstream/10803/403983/1/MNM_PhD_ THESIS.pdf.
Nebot, M., Guimerà, J., 2016. Structure of an inverted basin from subsurface and field data: the late Jurassic-early Cretaceous Maestrat basin (Iberian chain). Geol. Acta 14, 155–177.
Okay, A.İ., Demirbağ, E., Kurt, H., Okay, N., Kuşçu, İ., 1999. An active, deep marine strike-slip basin along the North Anatolian fault in Turkey. Tectonics 18, 129–147.
Okay, A.İ., Kaşlılar-Özcan, A., İmren, C., Boztepe-Güney, A., Demirbağ, E., Kuşçu, İ., 2000. Active faults and evolving strike-slip basins in the Marmara Sea, northwest Turkey: a multichannel seismic reflection study. Tectonophysics 321, 189–218.
Pardo, G., Villena, J., González, A., 1989. Contribución a los conceptos y a la aplicación del análisis tectosedimentario. Rupturas y unidades tectosedimentarias como fundamento de correlaciones estratigráficas, vol. 2. Revista de la Sociedad Geológica de España, pp. 199–219.
Pérez, A., 1990. Estratigrafía y sedimentología del terciario del borde meridional de la depresión del Ebro (sector riojano-aragonés) y cubetas de Muniesa y Montalbán, PhD thesis. Universidad de Zaragoza.
Pérez, A., Pardo, G., Villena, J., González, A., 1983. Estratigrafía y sedimentología del Paléogeno de la cubeta de Montalbán, prov. de Teruel, España. Boletín de la Real Sociedad Española de Historia Natural. Sección Geológica 81, 197–223.
Ringenbach, J.C., Pinet, N., Stéphan, J.F., Delteil, J., 1993. Structural variety and tectonic evolution of strike-slip basins related to the Philippine Fault System, northern Luzon, Philippines. Tectonics 12, 187–203.
Rodríguez-Pascua, M.A., De Vicente, G., 1998. Análisis de paleoesfuerzos en cantos de depósitos conglomeráticos terciarios de la cuenca de Zaorejas (Rama Castellana de la Cordillera Ibérica). Rev. Soc. Geol. Espana 11, 169–180.
Salas, R., 1987. El Malm i el Cretaci inferior entre el Massís de Garraf i la Serra d'Espadà: anàlisi de conca. PhD thesis. Universitat de Barcelona.
Salas, R., Casas, A., 1993. Mesozoic extensional tectonics, stratigraphy and crustal evolution during the Alpine cycle of the eastern Iberian basin. Tectonophysics 228, 33–55.
Salas, R., Guimerà, J., Mas, R., Martín-Closas, C., Meléndez, A., Alonso, A., 2001. Evolution of the Mesozoic central Iberian rift system and its Cainozoic inversion (Iberian chain). Mem. Mus. Natl. Hist. Nat. 186, 145–186.
Sato, K., Yamaji, A., 2006. Embedding stress difference in parameter space for stress tensor inversion. J. Struct. Geol. 28, 957–971.
Simón, J.L., 1981. Reactivación alpina del desgarre del Segre en el borde NE de la Cadena Ibérica. Teruel 65, 195–209.
Simón, J.L., 2004. Superposed buckle folding in the eastern Iberian Chain, Spain. J. Struct. Geol. 26, 1447–1464.
Simón, J.L., 2005. Erosion-controlled geometry of buckle fold interference. Geology 33, 561–564.
Simón, J.L., 2006a. El registro de la compresión intraplaca en los conglomerados de la cuenca terciaria de Aliaga (Teruel, Cordillera Ibérica). Rev. Soc. Geol. Espana 19, 163–179.
Simón, J.L., 2006b. Un protocolo de tratamiento estadístico para muestras polifásicas de lineaciones de disolución. Geogaceta 40, 67–70.
Simón, J.L., 2007. Analysis of solution lineations in pebbles: kinematical vs. dynamical approaches. Tectonophysics 445, 337–352.
Simón, J.L., 2019a. Forty years of paleostress analysis: has it attained maturity? J. Struct. Geol. 125, 124–133.
Simón, J.L., 2019b. Evolución de paleoesfuerzos registrada en la cuenca cenozoica de Montalbán (Teruel, Cordillera Ibérica). Geogaceta 66, 111–114.
Simón, J.L., Liesa, C.L., 2011. Incremental slip history of a thrust: diverse transport directions and internal folding of the Utrillas thrust sheet (NE Iberian Chain, Spain). Geological Society, London, Special Publications 349, 77–97.
Simón, J.L., Arlegui, L.E., Liesa, C.L., 2008. Stress partitioning: a practical concept for analysing boundary conditions of brittle deformation. Geodin. Acta 21, 107–115.
Simón, J.L., Liesa, C.L., Soria, A.R., 2018. Macizos del Maestrazgo, Gúdar y Javalambre. In: Alcalá, L., Calvo, J.P., Simón, J.L. (Eds.), Geología de Teruel. Instituto de Estudios Turolenses, Teruel, pp. 65–82.

Simón-Porcar, G., Liesa, C.L., Simón, J.L., 2019. La cuenca neógena extensional de El Pobo (Teruel, Cordillera Ibérica): sedimentología, estructura y relación con la evolución del relieve. Rev. Soc. Geol. Espana 32, 17–42.
Smit, J., Brun, J.P., Fort, X., Cloetingh, S.A.P.L., Ben-Avraham, Z., 2008. Salt tectonics in pull-apart basins with application to the Dead Sea Basin. Tectonophysics 449, 1–16.
Socquet, A., Pubellier, M., 2005. Cenozoic deformation in western Yunnan (China–Myanmar border). J. Asian Earth Sci. 24, 495–515.
Soria, A.R., Meléndez, A., Aurell, M., Liesa, C.L., Meléndez, M.N., Gómez-Fernández, J. C., 2000. The early Cretaceous of the Iberian basin (northeastern Spain). In: Gierlowski-Kordesch, E.H., Kelts, K.R. (Eds.), Lake Basins through Space and Time, AAPG Studies in Geology, vol. 46, pp. 257–262.
Sun, Z., Zhou, D., Zhong, Z., Zeng, Z., Wu, S., 2003. Experimental evidence for the dynamics of the formation of the Yinggehai basin, NW South China Sea. Tectonophysics 372, 41–58.
Sun, Z., Zhong, Z., Zhou, D., Qiu, X., Li, X., 2004. Continent-Ocean interactions within East Asian marginal Seas. Geophys. Monogr. 149, 109–120.
Sun, Z., Zhou, D., Zhong, Z., Xia, B., Qiu, X., Zeng, Z., Jiang, J., 2006. Research on the dynamics of the South China Sea opening: evidence from analogue modeling. Sci. China Earth Sci. 49, 1053–1069.
Sylvester, A.G., 1988. Strike-slip faults. Geol. Soc. Am. Bull. 100, 1666–1703.
Teixell, A., Barnolas, A., Rosales, I., Arboleya, M.L., 2017. Structural and facies architecture of a diapir-related carbonate minibasin (lower and middle Jurassic, High Atlas, Morocco). Mar. Petrol. Geol. 81, 334–360.
Vegas, R., de Vicente, G., Casas-Sainz, A., Cloetingh, S.A., 2019. Alpine Orogeny: intraplate deformation. In: Quesada, C., Oliveira, J.T. (Eds.), The Geology of Iberia: A Geodynamic Approach, The Alpine Cycle, vol. 3. Springer, Berlin, pp. 507–518.
Vergés, J., Poprawski, Y., Almar, Y., Drzewiecki, P.A., Moragas, M., Bover-Arnal, T., et al., 2020. Tectono-sedimentary evolution of Jurassic–Cretaceous diapiric structures: Miravete anticline, Maestrat basin, Spain. Basin Res. 32, 1653–1684.
Yamaji, A., 2000. The multiple inverse method: a new technique to separate stresses from heterogeneous fault-slip data. J. Struct. Geol. 22, 441–452.
Yang, Y., Chen, C., Wen, L., Chen, X., Liang, H., Liu, R., Xie, C., 2019. Characteristics of buried structures in northern Longmenshan mountains and its significance to oil and gas exploration in the Sichuan Basin. Nat. Gas. Ind. B 6, 175–182.
Žalohar, J., Vrabec, M., 2007. Paleostress analysis of heterogeneous fault-slip data: the Gauss method. J. Struct. Geol. 29, 1798–1810.
Zhihong, L., Hangjun, L., Peng, W., Xiangmei, W.U., Defeng, Z.H.U., Chuanbiao, W.A.N., 2009. Discovery of compressional structure in Wuerxun–Beier sag in hailar basin of northeastern China and its geological significance. Earth Sci. Front. 16, 138–146.
Audemard, F.A. (1995) Bassin Tertiaire de Falcon, Venezuela Nord-occidental: synthèse stratigraphique et inversion tectonique Mio-Quaternaire. 3Rd Geological conference of the Geological Society of Trinidad and Tobago, 570-583.
Martín-Chivelet, J., Xavier Berástegui, Idoia Rosales, Lorenzo Vilas, Juan Antonio Vera, Esmeralda Caus, Kai-Uwe Gräfe, Ramón Mas, Carmen Puig, Manuel Segura, Sergio Robles, Marc Floquet, Santiago Quesada, Pedro A. Ruiz-Ortiz, M. Antonia Fregenal-Martínez, Ramón Salas, Consuelo Arias, Alvaro García, Agustín Martín-Algarra, M. Nieves Meléndez, Beatriz chacón, José Miguel Molina, José Luis Sanz, José Manuel Castro, Manuel García-Hernández, Beatriz Carenas, José García-Hidalgo, Javier Gil, Francisco Ortega (2002). Cretaceous, In: The Geology of Spain, W. Gibbons, Teresa Moreno (eds.), Geological Society of London Special Publication, pp. 255-293.
Simón, J. L. (1982). Compresión y distensión alpinas en la Cadena Ibérica oriental, PhD Thesis. *Universidad de Zaragoza. Publ. Instituto de Estudios Turolenses, Teruel*.
Salas, R., Guimerà, J., 1996. Rasgos estructurales principales de la cuenca cretácica inferior del Maestrazgo (Cordillera Ibérica oriental). Geogaceta 20 (7), 1704–1706.